THE NITROGEN ION LASER

Carl B. Collins

Texas University at Dallas

Prepared for:

Office of Naval Research

31 December 1975

(1)

THE NITROGEN ION LASER

by

C. B. COLLINS

Seventh
Semi - Annual Technical Report
UTDP - ML - 04
prepared for
Office of Naval Research
Department of the Navy
sponsored by
Advanced Research Projects Agency

December 1975

SECURITY CLASSIFICATION OF THIS PAGE (When Data Entered)

REPORT DOCUMENTATION PAGE		READ INSTRUCTIONS BEFORE COMPLETING FORM
1. REPORT NUMBER UTDP ML-04	2. GOVT ACCESSION NO.	3. RECIPIENT'S CATALOG NUMBER
4. TITLE (and Subtitle) THE NITROGEN ION LASER		5. TYPE OF REPORT & PERIOD COVERED Semi-Annual Technical Period Covered-7/1/75-12/31/76 6. PERFORMING ORG. REPORT NUMBER
7. AUTHOR(s) Carl B. Collins		8. CONTRACT OR GRANT NUMBER(s) N00014-76-C-0174
9. PERFORMING ORGANIZATION NAME AND ADDRESS The University of Texas at Dallas P. O. Box 688 Richardson, Texas 75080		10. PROGRAM ELEMENT, PROJECT, TASK AREA & WORK UNIT NUMBERS NR 016 [illegible] ARPA Order No. 1807
11. CONTROLLING OFFICE NAME AND ADDRESS Office of Naval Research Department of the Navy Arlington, Virginia		12. REPORT DATE 31 December 1975 13. NUMBER OF PAGES ~~71~~ 73
14. MONITORING AGENCY NAME & ADDRESS(if different from Controlling Office) Code 421		15. SECURITY CLASS. (of this report) UNCLASSIFIED 15a. DECLASSIFICATION/DOWNGRADING SCHEDULE

16. DISTRIBUTION STATEMENT (of this Report)

Distribution of this document is unlimited

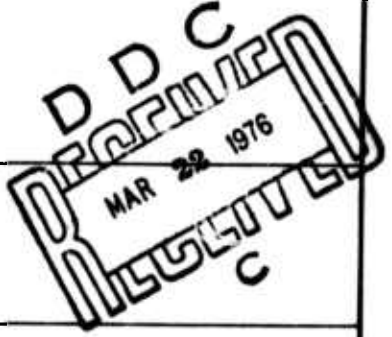

17. DISTRIBUTION STATEMENT (of the abstract entered in Block 20, if different from Report)

List of all receiving, per contractual requirements:
Semi Annual Technical Item No. A002

18. SUPPLEMENTARY NOTES

19. KEY WORDS (Continue on reverse side if necessary and identify by block number)

Nitrogen Ion Laser
Charge Transfer
Laser

20. ABSTRACT (Continue on reverse side if necessary and identify by block number)

The characterization and thermal scaling of the nitrogen ion laser pumped by charge transfer from He_3^+ is reported in this work. Intense laser emission in the violet at 427 nm has been observed and found to have a linewidth less than 0.3 Å. The pumping ion, He_3^+, was produced by discharge of a fast-pulsed electron beam gun, APEX-1, into several atmospheres of a mixture of helium and nitrogen. Excitation current densities ranged from 1.1 to 2.5 KA/cm^2 at 1 MV over a 1 x 10 cm transverse geometry. Under

DD FORM 1 JAN 73 1473 EDITION OF 1 NOV 65 IS OBSOLETE

SECURITY CLASSIFICATION OF THIS PAGE (When Data Entered)

these conditions, the efficiency of the emission of 427 nm laser radiation was found to be proportional to the total pressure raised to the 1.2 power. Efficiencies of 1.6% relative to the energy lost by the electron beam in the radiating volume have been achieved in volumes of 16 cc at room temperature. Outputs of 35 mJ have been obtained from the 16 cc working volume at 30 atm pressure under these conditions. Thermal scaling of the laser has been investigated and a strong inverse dependence of laser output on gas temperature was observed. At -20^{0}C the output was found to increase to 80 mJ from the 16 cc. volume containing helium at a density giving a pressure of 35 atm. at room temperature. This corresponded to an output efficiency of 3% relative to the energy deposited by the electron beam. Quasi-cw operation was achieved under these conditions suggesting that much longer output pulses might be obtained with an e-beam pulse of greater duration.

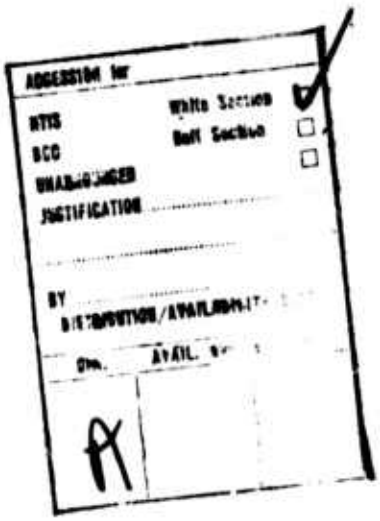

First Semi-Annual Technical Report

Item A002

Period Ending: 31 December 1975

Short Title: RECOMBINATION LASER

ARPA Order Number 1807

Program Code Number 2E90

Contract Number N00014-76-C-0174
Continuation of N00014-67-A-0310-0007

Principal Investigator: Carl B. Collins
Center for Quantum Electronics
The University of Texas at Dallas
P. O. Box 688
Richardson, Texas 75080
(214) 690-2863

Contractor: The Board of Regents of
The University of Texas System

Scientific Officer: Director
Physics Programs
Physical Sciences Division
Office of Naval Research
Department of the Navy
800 N. Quincy Street
Arlington, Virginia 22217

Effective Date of Contract: 1 July 1975

Expiration Date of Contract: 30 September 1976

Amount of Contract: $150,000.00

Sponsored by

Advanced Research Projects Agency

ARPA Order No. 1807

Form Approved Budget Bureau No. 22-R0293

CONTENTS

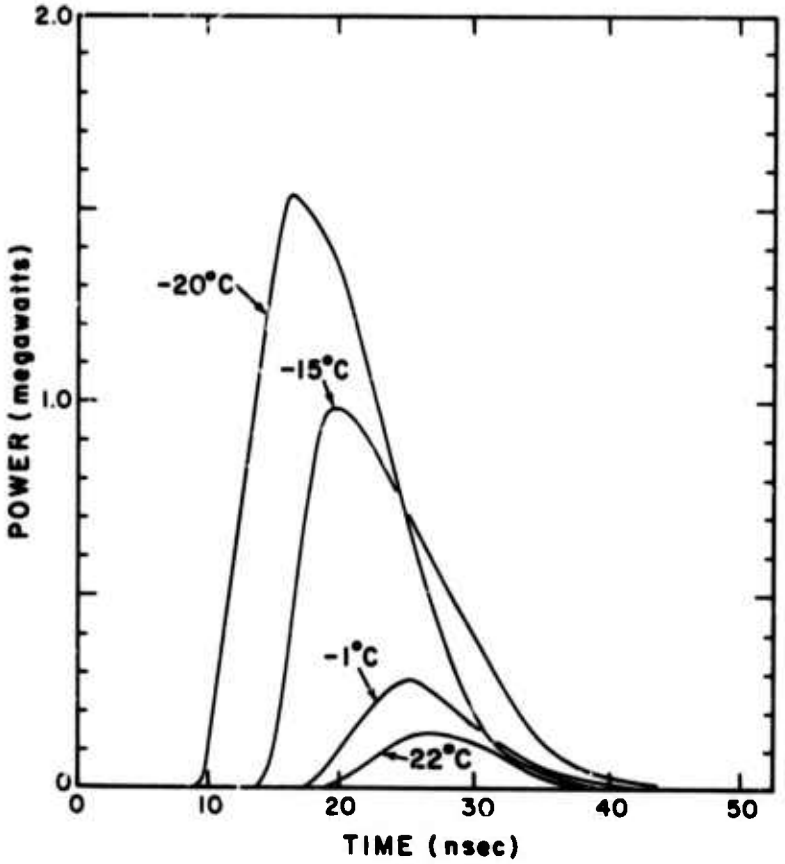

Figure 1: Thermal scaling of the helium-nitrogen charge transfer laser. Plotted parametrically as a function of gas temperature are time resolved power measurements of the violet line at 4278 Å. Data are shown for the discharge of 190 μ coulomb into 21 atm. pressure of helium containing 60 Torr of nitrogen. The time scale has been normalized so that the zero corresponds to the beginning of the e-beam current output.

I. TECHNICAL REPORT SUMMARY

The objective of the research pursued under this contract is to determine the feasibility of developing a high pressure helium plasma into a collisionally pumped laser emitting in the visible or near UV with 10 - 20% efficiency. Currently accepted theory[1,2,3,4] supported by the experimental results obtained to date under this contract indicate this to be a realistic goal. In fact, recent theoretical refinements[5,6] have led to increased, not decreased, estimates of photon yields. Experimental scaling studies of the helium-nitrogen charge transfer laser have tended to confirm this and the detailed kinetic model being developed continues to indicate this objective to be an attainable goal.

The power output pumped by the helium-nitrogen charge transfer sequence has been found[7,8] to scale at a rate showing a strong non-linear dependence on total gas pressure. This has necessitated a re-evaluation and subsequent refinement of the kinetic model of the pumping sequence, during the current reporting period. New terms involving previously unobserved processes, strongly dependent upon temperature, were included in order to bring theoretical predictions into agreement with performance observed at room temperature. Of most significance is that the new kinetic sequence suggested the scaling of laser output with decreasing temperature. Confirmation of this has now been obtained with the data presented in Figure 1 on the facing page. Over a twenty-fold increase in laser output has been achieved at low excitation currents for a 40°C decrease in temperature and

a two-fold increase in "best efficiency" has already been achieved.

When the helium-nitrogen charge transfer laser was first proposed by Collins et.al.,[9] in the course of work under the prior contract it was expected that the inverting transition in N_2^+ would be pumped by the resonant transfer of energy from the diatomic helium ion, He_2^+. Laser output was first achieved in high pressure plasmas excited by election beam discharges[10] and tended to confirm this, as did subsequent studies of scaling.[8] However, as inferred above, the parameterization of the efficiency of the laser output proved difficult to reconcile with the simple kinetic model first advanced. Data measured over a wide range of experimental parameters were found to be closely approximated by the empirical expression for the efficiency

$$\varepsilon = 6.5\%(P/100)^{1.2} \quad , \qquad (1)$$

where P was the total gas pressure in atmospheres and 6.5% was the theoretical limit on efficiency.[8] The validity of (1) was confirmed over a range of efficiencies varying from 0.3 to 1.6% as a consequence of changes in total pressure, fractional composition and mirror reflectivity. However, the first data from a program, initiated during the current reporting period, concerned with the measurement of the rate coefficients of the elementary reactions involved in the pumping sequence suggested that additional pumping steps were involved. Details of these results are presented in Section II together with a summary of rate coefficients obtained. They suggested, a posteriori, the importance of the formation of helium ion clusters and their subsequent

involvement in the reaction chain.

Unfortunately, little information about any of the inert gas ion-clusters is available in the literature, but both theory[11] and experiment[12] agree that such clusters are stable, at least in the case of He_3^+ and He_4^+. Most of the available information on helium ion clusters has been obtained from drift tube experiments[11] conducted in relatively tenuous plasmas at temperatures below 200°K and at pressures of the order of 10 - 20 Torr. If these low pressure results are extrapolated over two and a half orders of magnitude to 10 atmospheres pressure of helium, even at 300°K, 11% of the helium ion concentration can be expected to be triatomic. This, then, suggests the need to represent the pumping sequence of the helium nitrogen laser more generally as follows:

$$He^+ + 2He \rightarrow He_2^+ + He \qquad (2a)$$

$$He_2^+ + 2He \rightleftarrows He_3^+ + He \qquad (2b)$$

$$He_3^+ + 2He \rightleftarrows He_4^+ + He \qquad (2c)$$

$$He_n^+ + N_2 \rightarrow N_2^+(B^2\Sigma_u) + nHe \qquad (2d)$$

$$N_2^+(B^2\Sigma_u) + h\nu \rightarrow N_2^+(X^2\Sigma_g) + 2h\nu \quad , \qquad (2e)$$

where $n \geq 2$.

If it is then assumed, 1) that the inversion resulting from (2d) is pumped primarily by He_3^+, 2) that reaction (2b) is sufficiently fast that the concentration of He_3^+ is in thermal equilibrium with the He_2^+

after a few nanoseconds and 3) that one photon per He_3^+ is ultimately extracted by the fields in the laser cavity, then the expected laser output is in excellent agreement with the reported data as shown in Figure 2. The 47°C temperature corresponds to the value reasonably expected in a helium sample, initially at room temperature, heated by a 20-30 nsec. 1 MeV electron beam pulse of 275 μ coulomb as used in these experiments.

The laser device and experimental details involved in this work have been described previously[7-10] and will be reviewed only briefly in Section IIIA for convenience. In operation three laser lines have been excited in mixtures of helium (1-35 atm) and nitrogen (2-120 Torr) pumped by reaction (2). Each corresponds to transitions from the same upper vibrational state, v = 0, of the $B^2\Sigma_u^+$ electronic state to different lower vibrational states of the $X^2\Sigma_g^+$ electronic state of the N_2^+ molecular ion. The three lines and their respective vibrational transitions are: the 3914 Å (0,0), the 4278 Å (0,1), and the 4709 Å (0,2). With the proper mirror set, each has been excited individually. The most work has been done on the (0,1) transition at 4278 Å, but since each has the same upper state, those same results should be roughly characteristic of all with the exception of the (0,0) transition which self-terminates at very early times. The dependence found for the output pulse energy on gas pressure and hence deposition was shown in Figure 2. The dependence on e-beam current, however, was much less than linear and showed a type of saturation between 15 and

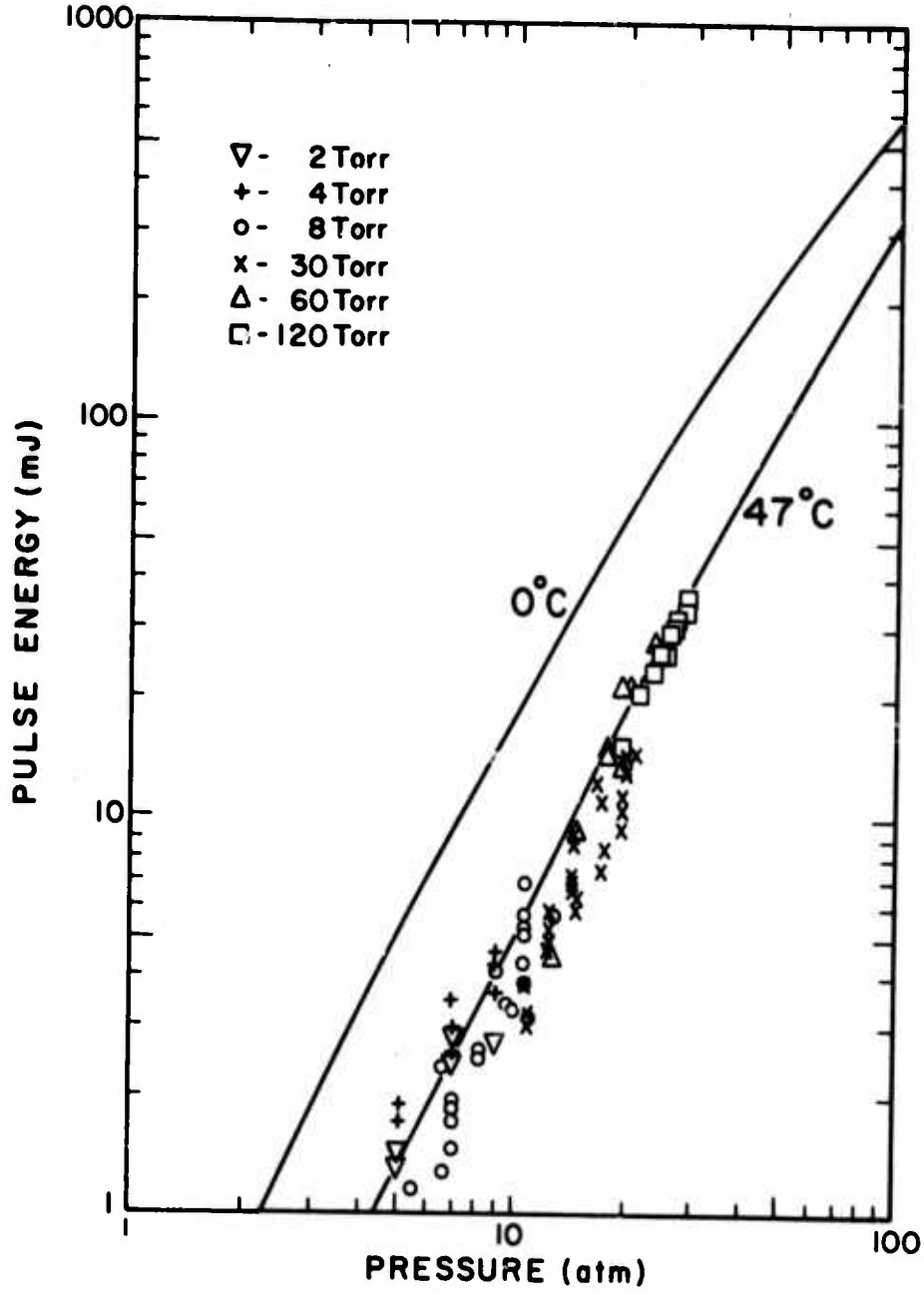

Figure 2: Summary plot of total laser pulse energy emitted from a 16 cm^3 volume as a function of total gas pressure. The integrated e-beam current corresponds to 275 μ coulomb for each case. Data points represent output at 4278 Å and different partial pressures of N_2 are indicated by the shape of the data point as follows, except for + and ▽; O - 8 Torr, X - 30 Torr, Δ - 60 Torr, □ - 120 Torr. The + and ▽ symbols plot the total pulse energy extracted at 3914 Å from the plasma by the fields in the cavity and have been corrected for reabsorption at the end of the pulse. Solid curves plot theoretical predictions of the kinetic model described by eqns. (2a) - (2e) for the average gas temperatures indicated.

25KA which made analysis in terms of time integrated current more attractive. Below 15KA the laser output was found to be strongly dependent upon beam current and under these conditions the most pronounced dependence on gas temperature was expected.

Figure 1 showed the effect of cooling the gas prior to the electron beam discharge at a current of 11KA and factors of improvement as large as 20 were obtained in the energy emitted in the laser pulse for a 40°C decrease in the initial average gas temperature. Though not as remarkable as the effects on the unsaturated laser outputs shown in the figure, the effects of a similar decrease in temperature on discharges at higher currents and pressures were substantial. "Best" outputs at each pressure were increased by a factor of approximately 2 for a 40 to 50°C decrease in average gas temperature. A peak power of 5.2 Megawatt at 4278 Å was obtained at an average gas density corresponding to a pressure of 35 atmospheres at room temperature. The corresponding pulse energy was 80mJ and represented an output efficiency of 3% relative to the energy deposited by the electron beam. As discussed in Section IIIC, data obtained over a range of pressures and gas compositions was found to fit the following empirical expression for the efficiency over the 10 - 35 atm pressure range examined,

$$\varepsilon(-20°C) = 10.5\%(P/80)^{1.2} \quad , \qquad (3)$$

where P is the equivalent gas pressure at room temperature, as in the

expression for the efficiency at room temperature, eq. (1), and 10.5% is the revised theoretical limit on efficiency.

An additional benefit accrued during the operation at lower temperature in that quasi - cw operation of the laser was achieved at 4278 Å. Output power was found to accurately follow input power after onset of threshold. Data shown in Figure 3 is typical of the close correlation of output power with a constant percentage of power input to the lasing volume, in this case at the 3% level. Such operation is believed to confirm the importance of the capture-autoionization sequence for the relaxation of vibrational energy in the lower laser level,

$$N_2^+(X^2\Sigma_g)_{v=1} + e \rightarrow N_2^{**}{}_{,v=1} \quad , \tag{3a}$$

$$N_2^{**}{}_{,v=1} \rightarrow N_2^+(X^2\Sigma_g)_{v=0} + e \quad , \tag{3b}$$

where the double asterisk indicates an autoionizing level.

In summary, then, it appears that step (2d) is pumped primarily by He_3^+, as is indicated by the excellent agreement of the model with the room temperature results presented in Figure 2. Such a model not only is able to explain the strongly non-linear dependence on gas pressure of the energy of the output pulse of the laser, but also has succeeded in predicting a strong inverse dependence on gas temperature, subsequently confirmed by the work reported in detail in Section IIIC. It is, then, consistent

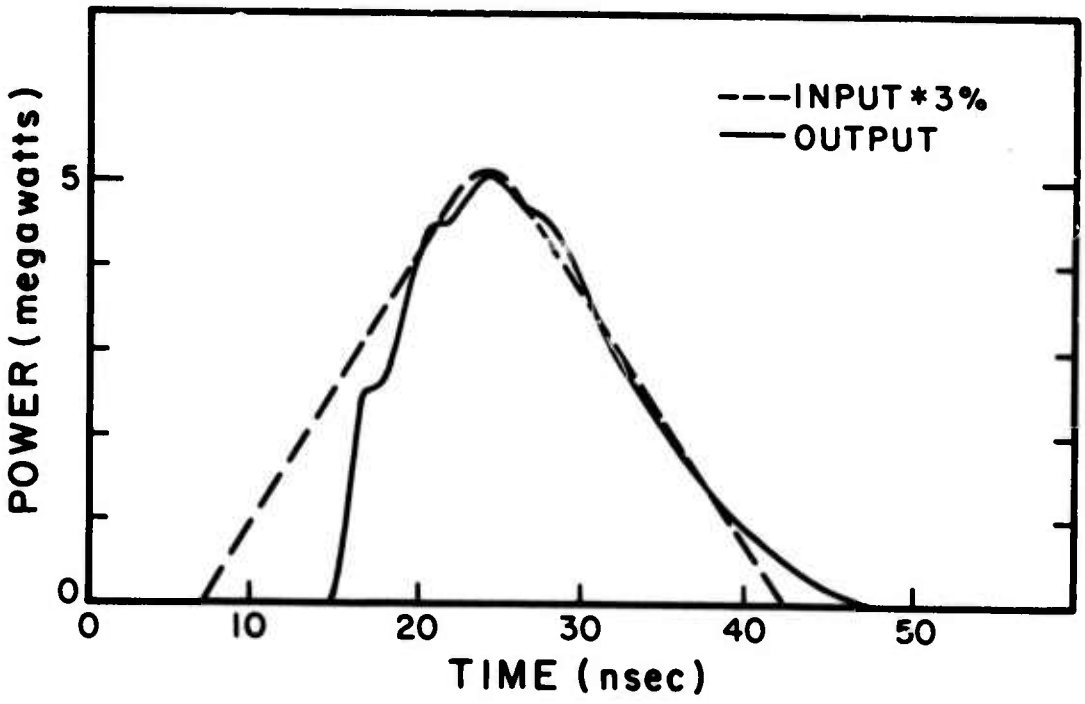

Figure 3: Plot of data showing quasi-cw operation of the helium-nitrogen laser. The solid curve shows output power at 4278 Å emitted from an electron beam discharge into 35 atmospheres pressure of helium containing 120 Torr of nitrogen. The dashed curve shows 3% of the corresponding power deposited in the laser cavity.

with this model to expect that the proper choice of temperature and pressure will favorably adjust the equilibrium ratio of He_3^+ to He_2^+ so that the theoretical limit on efficiency of the helium nitrogen charge transfer laser of 6 to 10% can be closely approached.

While it should be realized that the nitrogen ion laser is only the first example of the new class of e-beam charge-transfer lasers,[9] and that other similar systems offer the possibilities of even higher efficiencies and broader selections of output wavelengths, these results observed for the emission of 4278 Å laser radiation point to the nitrogen ion laser as a device of considerable significance and clearly confirm the importance of charge transfer reactions as laser pumping mechanisms.

II. THEORY AND RATE COEFFICIENTS OF ELEMENTARY REACTIONS

The development of intense pulsed electron beam sources in the 1 to 100 Gigawatt class have made feasible the deposition of energy in the form of ionization into large volumes of plasma with system efficiencies around 50%. These devices can be used alone to excite laser plasmas or can be combined at reduced intensities with sustained excitation at the proper E/p to store large densities of energy in high pressure inert gas systems. The quantum of energy storage is characteristically large in the inert gases and ranges from 10 to 20 eV. Given an elementary mechanism utilizing this stored energy and leading to the inversion of population, overall radiative efficiencies of the order of 10 to 20% can be realistically projected, provided the plasma constituents are arranged to allow for the domination of the desired reaction channel.

The objective of the research reported here has been to determine the feasibility of developing a high pressure helium plasma into a collisionally pumped laser emitting in the visible or near UV with an efficiency in the range of 10 - 20%. However, the problems of the practical excitation of the plasma itself have been deferred until a later stage of the research and plasmas actually studied have been ionized directly by an electron beam of high intensity. Instead, the primary emphasis of this work has been placed on the understanding of the basic physics of possible kinetic sequences of importance and of their characteristic coupling to the electro-

magnetic field in a laser cavity.

The concept of the collisional pumping of ion transitions in e-beam plasmas was first proposed by Collins et.al.[9] in the course of work under this contract. The first example to be realized in this wholly new class of e-beam lasers was the nitrogen ion laser[10] pumped by charge transfer from He_2^+ as announced in 1974. In this class of pumping reactions are the related processes of charge transfer, Penning ionization, and recombination. It appears, a priori, that these mechanisms represent the most efficient means of exploiting, for the production of visible laser radiation, the energy stored in a high pressure gas by an intense electron beam. Since over 80% of the energy of a relativistic electron beam can be stored either as ionization or metastables in the volume of high pressure helium, these elementary mechanisms for using this stored energy to produce an inversion of population makes possible particularly high overall efficiencies. A value approaching that of the absolute quantum efficiency of the transition can be expected.

Charge transfer offers considerable advantages over other laser pumping mechanisms because of the large cross sections, 10^{-14} cm^2, characteristic of such processes. These values lead to reaction rates which are at least an order of magnitude larger than those characteristic of most excitation transfer sequences involving neutral atomic and molecular species. As a consequence, in most cases considered, charge transfer can be readily

arranged to be the dominant process for loss of the ionization deposited by the electron beam or other discharge device. This can be done with relatively small concentrations of the gas to be excited which in turn, means that chemical quenching of the final excited state population should be virtually negligible, as seems to be the case in the nitrogen ion laser.[6,7] For example, only 30 Torr of N_2 represents the optimum concentration in 20 atm. of helium. Secondary advantages lie in the larger number of possible reaction systems making probable a larger selection of transition wavelengths.

Theory supported by observations of fluorescence resulting from charge transfer and Penning ionization reactions[13] indicate these are resonant processes. Figure 4 shows a typical energy level diagram from which the resonances of the ions of helium with the upper state of the nitrogen ion laser transition, the $B^2\Sigma_u$ state of N_2^+ can be readily appreciated. Unfortunately, little information about any of the inert gas ion clusters is available in the literature, but both theory[11] and experiment[12] agree that such clusters are stable, at least in the case of He_3^+ and He_4^+. Most of the available information on helium ion clusters has been obtained from drift tube experiments[12] conducted in relatively tenuous plasmas at temperatures below 200°K and at pressures of the order of 10 - 20 Torr. Nevertheless, if these low pressure results are extrapolated over two and a half orders of magnitude to 10 atmospheres pressure of helium, even at 300°K, 11% of the helium ion concentration can be expected to be in the form

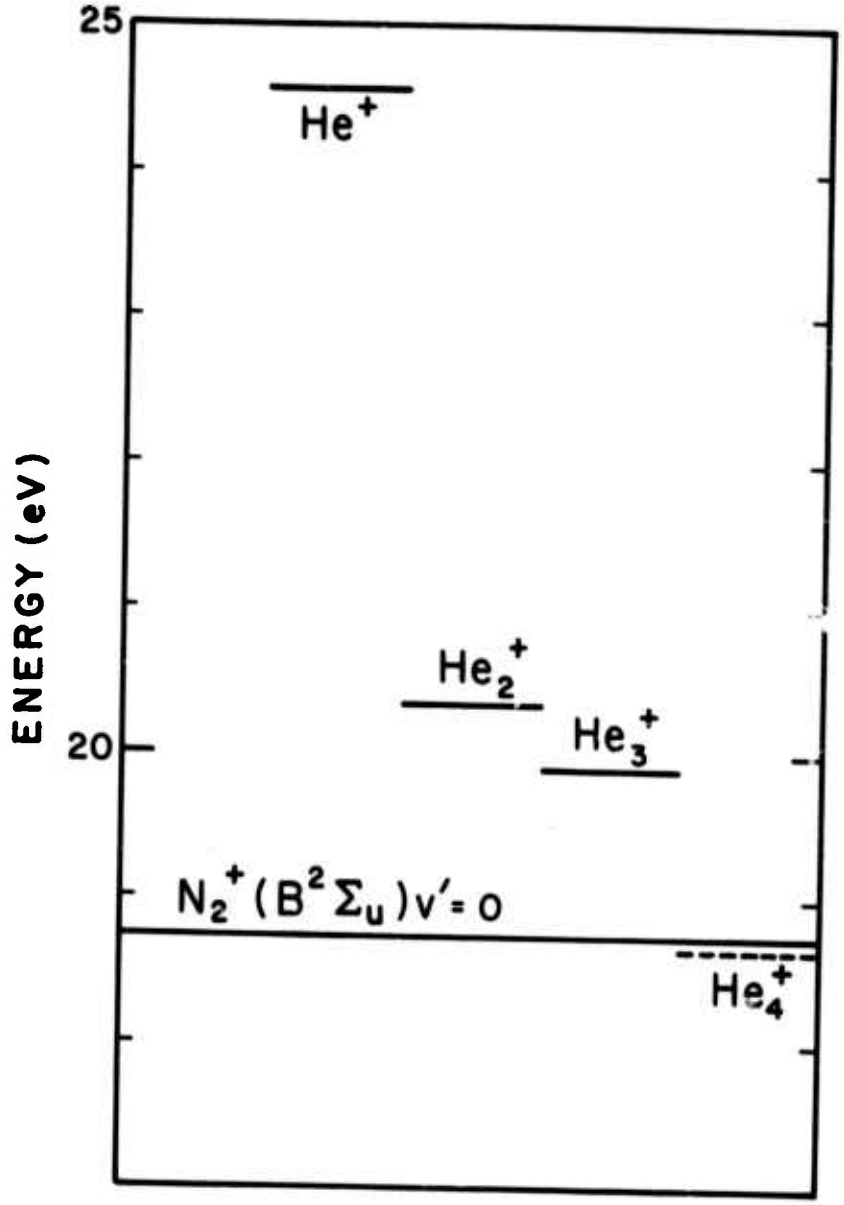

Figure 4: Energy level diagram comparing the most probable energy available for transfer from the helium ions indicated with the excitation energy of the $v' = 0$ level of the $B^2\Sigma_u$ state of N_2^+. Uncertainty in the available energy of the He_4^+ ion is suggested by the dashed line.

of He_3^+. Although the dissociation energy of He_3^+ has been measured to be 0.17eV, and so relatively little energy is lost in successively binding additional helium atoms to the He_2^+ ion, the energy available for transfer is reduced substantially because of the repulsive energy between pairs of neutral helium atoms[14] remaining at small internuclear separations after any transfer reaction. This tends to bring a closer resonance with the $v' = 0$ level of the B state of N_2^+ for He_3^+ than for He_2^+ and precludes the reaction of He_4^+ with N_2, making it endothermic as seen in Figure 4. These considerations then suggest the necessity of including the kinetics and energetics of the ion aggregates in any hypothetical pumping sequences. Further, due to the similarity of the available energies of the He_3^+ ion and the 2^3S metastable, it can be expected[13] that reaction products from charge transfer with He_3^+ and from Penning ionization with $He(2^3S)$ will be largely indistinguishable. In that case, the populations of He_3^+ ions and 2^3S metastables can be realistically grouped together as pumping species in kinetic models. While the energy cost to produce an ion in helium directly, is 42.3 eV, the cost is significantly lower, 27.8 eV, to produce ionization from the total population of ions and metastables.[15] These realizations have led to the "recent" increase in the efficiency expected for collisional pumping mechanisms used in Section IV. Table 1 summarizes examples of resulting system efficiencies possible for the various permanent gases diluted in helium.

TABLE I

Projected system efficiencies for the emission of radiation following charge transfer and Penning ionization from helium for the output wavelengths shown.

Minor Constituent	Wavelength	Overall Efficiency
N_2	4278 Å	10.5%
CO_2	2900 Å	15%
CO	2300 Å	19.5%

The development of a comprehensive kinetic model of the reaction sequences of possible importance in high pressure helium plasmas has been impeded by the paucity of appropriate kinetic data in the literature. Consequently, a program was initiated during the current reporting period concerned with the measurement of the rate coefficients for the reaction of ions found to be abundant in the higher pressure plasmas.

Reactions of interest were those binary reactions serving to transfer the stored energy into excitation of a product state capable of supporting the extraction of stimulated emission. Such reactions of the type,

$$He_n^+ + X \rightarrow n\,He + (X^+)^*, \qquad (4)$$

where n = 1 or 2, or 3, X is the reacting additive and $(X^+)^*$ is the product state, can be described by a binary rate coefficient k, so that the rate

of conversion of the energy storing species is

$$-\frac{d}{dt}[He_n^+] = k\,[He_n^+][X] \quad , \tag{5}$$

where the brackets denote concentrations. Techniques for determining values of the reaction coefficient, k, must depend upon measurement of product population, $(X^+)^*$ or reactant population, He_n^+. Measurements of the latter can be either direct, through techniques of optical absorption, or indirect through detection of spontaneous radiation from products of some other reaction involving the primary species since the primary species itself cannot radiate.

A satisfactory technique for the detection of the He_2^+ concentration has been found[16] to be the measurement of spontaneous radiation at 6400 Å resulting from the recombination of this ion with elections. In a pure, helium plasma the rate equation for the He_2^+ ion can be expressed as

$$\frac{d}{dt}[He_2^+] = k_s[He^+][He]^2 - \alpha(e)[He_2^+][e] \tag{6}$$

where k_s is the rate coefficient for the formation of He_2^+ by the termolecular reaction of He^+ with two neutral helium atoms, (2a) and $\alpha(e)$ is the recombination rate coefficient of He_2^+ with elections. Due to rapid conversion of He^+ to He_2^+, the source term of He_2^+ may be neglected after a

few nanoseconds and equation (6) may then be expressed as

$$\frac{1}{[He_2^+]}\frac{d}{dt}[He_2^+] = -\alpha(e)[e] \qquad (7)$$

or as

$$-\frac{d}{dt}(\ell n[He_2^+]) = \alpha(e)[e] \equiv \nu(t) \qquad (8)$$

where $\nu(t)$ is defined to be the destruction frequency of the ions due to recombination.

However, the electron concentration is also a function of time and may be similarly expressed as

$$-\frac{d}{dt}(\ell n[e]) = \nu_e(t) \qquad (9)$$

where $\nu_e(t)$ is the corresponding destruction frequency or inverse lifetime of the electron concentration in the plasma. Equation (8) may then be combined with equation (9) in the form

$$-\frac{d}{dt}(\ell n[e]+\ell n[He_2^+]) = -\frac{d}{dt}(\ell n[He_2^+][e]) = \nu(t) + \nu_e(t) \quad . \qquad (10)$$

The product of $[He_2^+][e]$ can be related to the intensity of the 6400 $\mathring{A}$ emission by a constant, $C = hc\,\nu_{6400}\,A_{6400}\,f\,G$, where f is the fraction of recombination events leading to formation of a $d^3\Sigma$ molecule radiating the 6400 $\mathring{A}$ line, ν is the wave number of the radiation, G is the geometric

factor for the total efficiency of the detection system, and A is the Einstein A- coefficient for the transition. Therefore,

$$- \frac{d}{dt}(\ell n \frac{1}{C} [I_{6400}]) = \nu(t) + \nu_e(t) \quad . \qquad (11)$$

When a second gas is added to the helium plasma, equation (11) takes the form

$$- \frac{1}{\tau_{exp}} \equiv - \frac{d}{dt}(\ell n \frac{I}{C}[I_{6400}]) = \nu_o(t) + \nu_e(t) + k[A] \qquad (12)$$

where k is the rate coefficient for the binary reaction of the He_2^+ ion with the additive species A. The left-hand side of equation (12) is an expression for the inverse lifetime of the 6400 Å intensity which can be determined experimentally from the transient dependence of the 6400 Å fluorescence following the termination of the e-beam discharge.

Figure 5 shows typical fluorescent decays of the 6400 Å radiation for several values of partial pressure of the CO additive. The inverse lifetime, $(\tau_{exp})^{-1}$ appearing in eq. (12) is the slope of the linear approximation to the curve. Taking the partial derivative of equation (12) with respect to the concentration of A gives an expression for the rate coefficient for the reaction of the He_2^+ ion with the additive A in terms of experimentally measured intensity.

$$\frac{\partial}{\partial [A]} \left(\frac{d}{dt}(\ell n \frac{1}{C} [I_{6400}])\right) = -k \qquad (13)$$

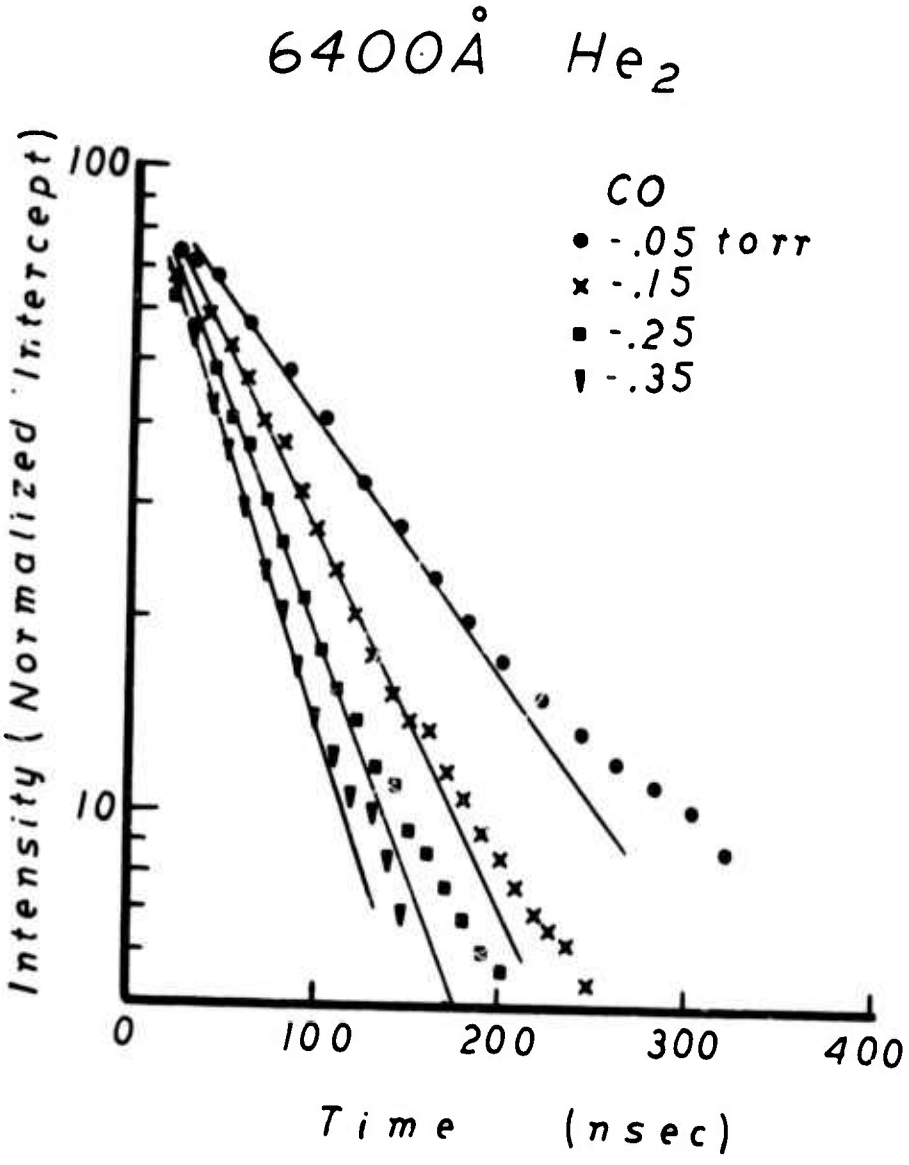

Figure 5: Data showing the decay of the logarithm of the intensity of the spontaneous emission detected at 6400 Å as a function of time and, parametrically, as a function of partial pressure of admixed CO.

This is a standard procedure in chemistry and such a Stern-Volmer plot has the characteristics shown in Figure 6 for the data of Figure 5 for the reaction of He_2^+ with CO. As shown, the slope of the curve in Figure 6 gives the charge transfer rate coefficient appearing in eq. (13) and provided the points representing the inverse lifetime at low partial pressures do not deviate critically from the line determining the rate coefficient, the intercept of this line gives the normal inverse lifetime for the He_2^+ population in pure helium.

Examination in an analogous manner of the transient dependence of the fluorescence from the product states of the reaction should give the same rate coefficient provided it is, in fact, He_2^+ transferring the energy and provided the radiative lifetime of the fluorescence is fast enough so that the product population "follows" the time dependence of the reacting population. This happens whenever the radiative lifetime is not the rate limiting step in the sequence of events producing the fluorescence. By analogy

$$-\frac{1}{\tau_p} \equiv -\frac{1}{dt}(\ell n[I_q]) = \nu_2(t) + K_p[A] \qquad (14)$$

where τ_p is the inverse lifetime of the fluorescence intensity, I_q, measured experimentally, $\nu_2(t)$ is the destruction frequency in pure helium and K_p is the rate coefficient of the transfer reaction producing the fluorescence. Constructing the analogous Stern-Volmer plot is sufficient to determine

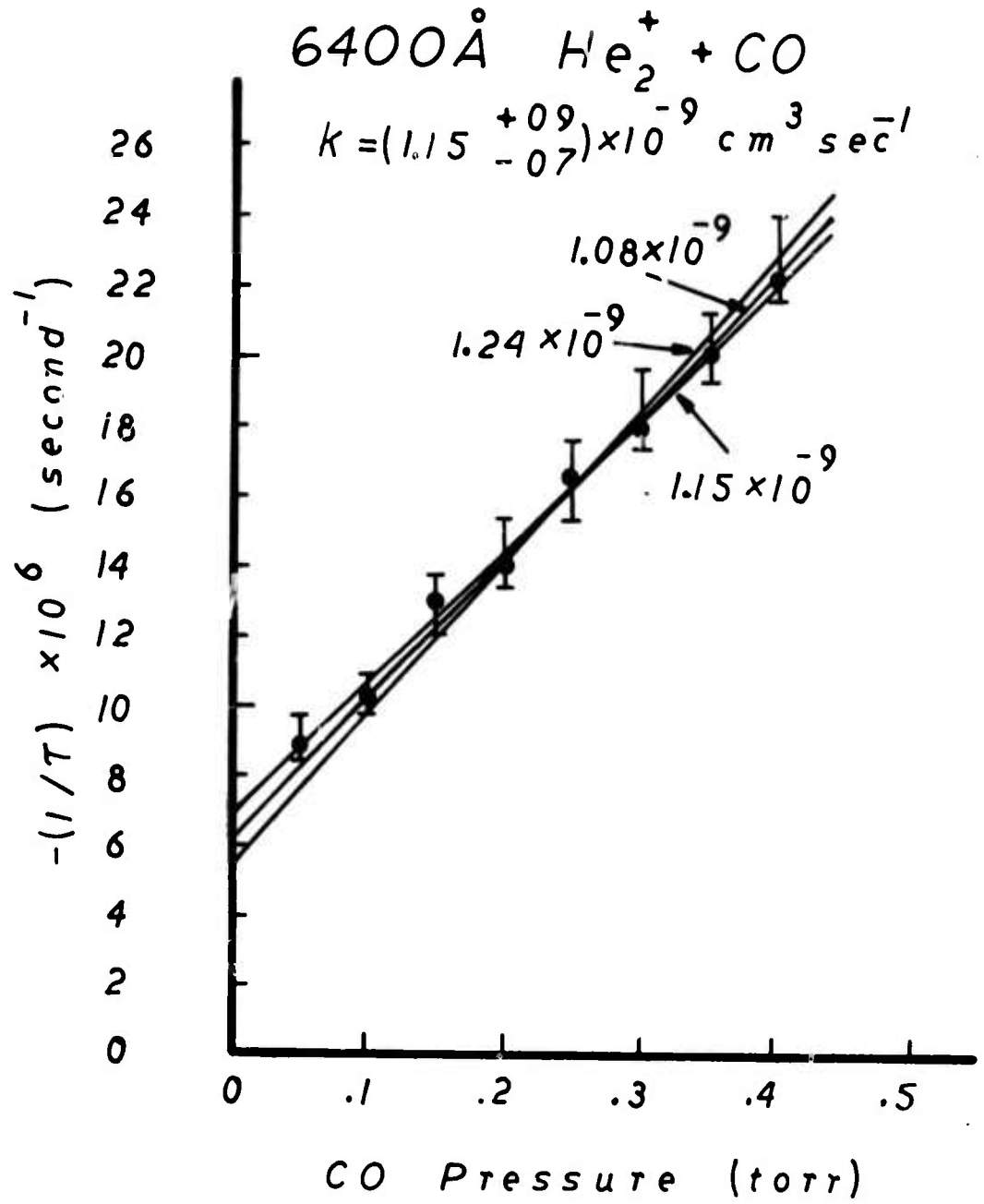

Figure 6: Stern - Volmer plot of the negative inverse lifetime of the 6400 Å spontaneous emission as a function of CO partial pressure.

K_p. For the particular fluorescence to be pumped by He_2^+ it is necessary that the resulting $K_p = K$. For example, in Figure 7 the Stern - Volmer plot obtained from the fluorescence of the Baldet - Johnson (B→X) bands of CO^+ is seen to yield a value of

$$K_p = 1.15 \times 10^{-9} \text{ cm}^3/\text{sec} \qquad (15)$$

in complete agreement with the value of K obtained from the data of Figure 6. It can be readily concluded that both measurements concerned the charge transfer reaction

$$He_2^+ + CO \rightarrow (CO^+)^* + 2He \qquad (16)$$

and that the corresponding rate coefficient has the value 1.15×10^{-9} cm^3/sec.

The only values for thermal energies of collision available in the literature for comparison are those from the ESSA group giving[17]

$$K(\text{ESSA}) = 1.4 \times 10^{-9} \text{ cm}^3/\text{sec} \quad , \qquad (17)$$

from data taken in a low pressure mass spectrometer experiment at 200^0K and the Bourene result[16] of

$$K(\text{Bourene}) = 5.3 \times 10^{-10} \text{ cm}^3/\text{sec} \quad , \qquad (18)$$

obtained from an experiment similar to the one reported here. However, the hot electrons in their experiment were magnetically confined and so could have complicated the interpretation of the 6400 Å radiation and rendered their interpretation somewhat equivocal. In any case, the results of this experiment agree with the mass spectroscopic results to within the limits of a possible temperature dependence of the rate coefficient. Further, the

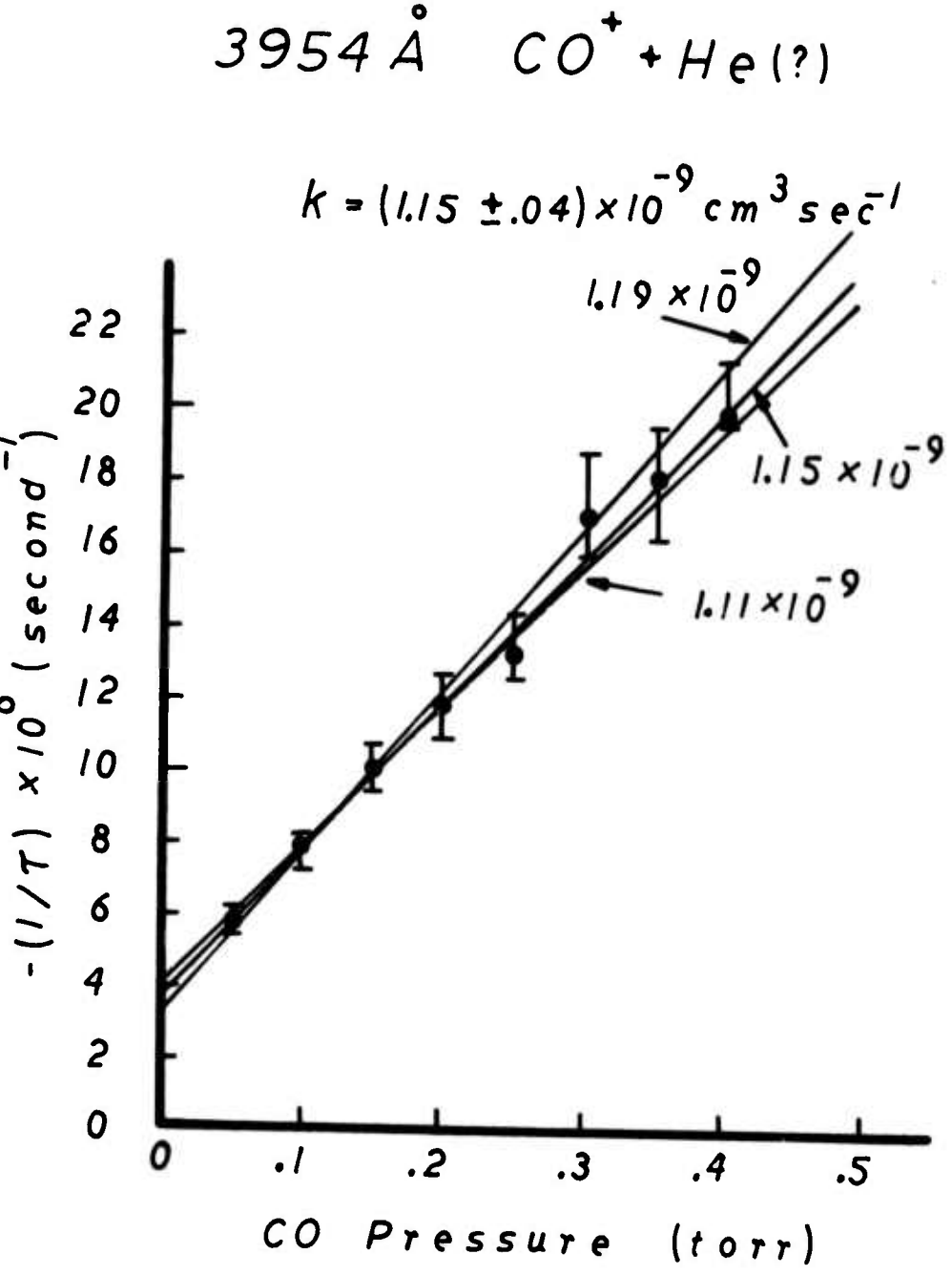

Figure 7: Stern - Volmer plot of the negative inverse lifetime of the 3954 Å spontaneous emission of CO^+ as a function of CO partial pressure in one atmosphere of helium.

agreement obtained here between reactant and product channels of the reactions strongly supports the results of these experiments. Such verification has not been reported in previous work.[16,17]

Such an agreement was not observed in the case of the helium-nitrogen charge transfer reaction. Rates for the following reactions were measured to be

$$He_2^+ + N_2 \rightarrow \text{Products} \quad , \qquad K = 1.3 \times 10^{-9} \text{ cm}^3/\text{sec} \qquad (19)$$

$$\text{Reactants} \rightarrow N_2^+(B^2\Sigma_u) + nhc \quad , \qquad K = 0.9 \times 10^{-9} \text{ cm}^3/\text{sec} \quad . \qquad (20)$$
$$\rightarrow \text{other branches}$$

The discrepancy is significantly greater than the experimental uncertainty and was verified to be reproduceable under a variety of experiment conditions. For this case the ESSA result was 1.3×10^{-9} cm^3/sec and strongly supports the value found for reaction (19) in this work. The most straightforward explanation of the difference is that some other ion is involved in the input channel of reaction, (20). From the energetics discussed above the most likely is He_3^+ suggesting that it is the charge transfer reaction

$$He_3^+ + N_2 \rightarrow N_2^+(B^2\Sigma_u) + 3He \quad , \qquad (21)$$
$$\rightarrow \text{other branches}$$

which is proceeding with the measured total rate coefficient

$$K = 0.9 \times 10^{-9} \text{ cm}^3/\text{sec} \quad , \qquad (22)$$

and which is responsible for the observed fluorescence from the $N_2^+(B^2\Sigma_u)$ state. To support this hypothesis several tests were made including observation of the necessary inverse dependence of fluorescence on temperature and the more comprehensive test discussed in the immediately following material.

If, indeed, He_3^+ is the dominant species pumping the nitrogen ion fluorescence then it should be possible to introduce a trace amount of nitrogen into a mixture of helium and a more abundant reactant and use the nitrogen fluorescence to monitor the reacting population of He_3^+ in a manner analogous to that in which the recombination radiation was used to monitor the reacting He_2^+ population. This was in fact accomplished during the current reporting period and has led to the first determination of charge transfer reaction rates involving He_3^+. The resulting tabulation is shown in Table 2 while Table 3 summarizes the results for He_2^+ in comparison with previous measurements.

TABLE 2

Summary of charge transfer rate coefficients obtained from these measurements for He_3^+ and He_2^+ with the reactants listed. Units are 10^{-10} cm^3/sec.

Reactant	He_3^+	He_2^+
N_2	9	12
CO	12	12
CO_2	17 ± 2	13
Ar	12	1.4
Ne	1.6	--

TABLE 3

Comparison of charge transfer rate coefficients for He_2^+ with various reactants measured in this work with previous values.

Reactant	This Work	ESSA[17]	SACLAY[16]	Villarejo[18]	Oskam[19]
N_2	12	13	6	2.2	
CO	12	14	5.3		
CO_2	13	18	12.5		
Ar	1.4	2.0	2.5		
Ne	1.6	6.0	1.5	1.2	1.5

Having this basic kinetic data available makes the construction of a comprehensive kinetic model relatively straightforward. First, at

sufficiently high pressure, the He^+ is rapidly converted to He_2^+ by the termolecular reaction

$$He^+ + 2He \rightarrow He_2^+ + He \qquad (23)$$

with a characteristic lifetime[20] of

$$\tau = \frac{27}{p^2} \text{ nsec} \qquad (24)$$

where p is in atmospheres. The subsequent conversion

$$He_2^+ + 2He \rightarrow He_3^+ + He \quad , \qquad (25)$$

has been estimated to proceed even more rapidly.[21] Provided the partial pressure of minority constituent is not too great for reactions (23) and (25) to go to completion, the ionization will convert from He^+ to He_3^+, thus making available the charge transfer reaction (21).

As summarized in Tables 2 and 3 the charge transfer reactions of both He_2^+ and He_3^+ with nitrogen have rate coefficients of the order of 10^{-9} cm^3/sec as does the analogous reaction[22] with He^+.

Requiring, then, a low enough partial pressure of nitrogen so that reactions (23) and (25) can reach an $(1-e^{-1})$ end-point yield in competition with the competing channel for the loss of He^+ and He_2^+ through unwanted charge transfer sets the upper limits on the partial pressures shown in Table 4.

TABLE 4

Partial pressures of He and diatomic admixtures to allow for a conversion of a fraction of $(1-e^{-1})$ of He^+ to He_2^+ in competition with charge transfer of He^+ and He_2^+ and the resulting charge transfer lifetimes.

He	Max Admixture	Charge Transfer Lifetimes
3 atm	5.9 Torr	5.3 nsec
30 atm	590 Torr	0.05 nsec

Determination of the actual output energy available in the resulting population of the $N_2^+(B^2\Sigma_u)$ state requires knowledge of the branching ratio between the possible output channels from the transfer reaction. It has been discussed in previous contract reports[7] that the occurrence of gain in the (0,0) vibrational component of the $N_2^+(B^2\Sigma_u \rightarrow X^2\Sigma_g)$ electronic transition requires at the minimum, 50% of the N_2^+ product population be pumped into the upper $B^2\Sigma_u$ state. The strength of the laser oscillations actually observed in this transition indicates, rather, that over 75-80%, and possible ~100%, of the product ions are in the upper $B^2\Sigma$ state. Thus it is reasonable to approximate the energy available in the product population as being potentially one output photon per He_3^+ ion. The fact that the dissociation energy of He_3^+ is only 0.17eV makes the inverse of reaction (25) probable and a kinetic equilibrium of He_3^+ and He_2^+ must be expected.

Since rates of reaction of both ions with nitrogen are virtually the same, adherence to the concentration limits of Table 4 will only insure that the equilibrium fraction of He_3^+ reacts to populate the inverting $B^2\Sigma$ level of N_2^+. To attain one photon per helium ion originally produced the equilibrium ratio of He_3^+ to He_2^+ must be shifted in favor of the desired ion.

Patterson[12] gives the equilibrium constant to be

$$\frac{[He_2^+][He]}{[He_3^+]} = 1.67 \times 10^{20} [1-\exp(-300/E)]^{-2} T^{3/2} \exp(-1371/E), \quad (26)$$

where T is the temperature and E is the kinetic energy in cm^{-1} corresponding to that temperature. As expected, both increasing pressure and decreasing temperature tend to increase the He_3^+ fraction and hence the efficiency of recovering one photon per ion originally produced.

It will be seen in the following section that expression (26) is sufficient to account for the pressure-dependent laser efficiency actually observed and to predict important thermal scaling effects verified in Section IIIC. Finally, it is important to recognize that other potentially limiting mechanisms such as quenching are minimized in the charge transfer scheme described here. In this fact lies the primary advantage in this mechanism. It results largely from the large cross sections, 10^{-14} cm^2, characteristic of such processes. These values for the charge transfer process are at

least an order of magnitude larger than those characteristic of most other excitation transfer reactions involving neutral atomic and molecular species. This means much smaller concentrations of the gas to be excited can be used which, in turn, means that chemical quenching of the final excited state population should be virtually negligible, as seems to be the case in the nitrogen ion laser actually realized.

III. THE NITROGEN ION LASER, PHENOMENOLOGY

As mentioned in the introductory section, it was first demonstrated almost two years ago[9] that resonant charge transfer held considerable promise as a potential laser pumping mechanism. Direct measurements of gain obtained with a tunable dye laser were reported at that time. Lasing was reported a few months later.[10] Outputs were small, 9 KW, but efficiencies were around 1.8%. However, excited volumes were quite small, 0.63 cm^3, and the first concern upon receipt of the electron beam source at our facility was to determine the scalability of this result to larger volumes more nearly corresponding to the use of the entire e-beam cross section.

The subsequent series of experiments reported[8] served to raise outputs to 325 KW and lower efficiencies slightly to 1.6%. Complicated effects resulting from the non-linearity of the reaction sequence tended to confuse the early phenomenology.

This report concerns the resolution of many of these effects. As has already been discussed in the preceeding technical report, output variation with mirror reflectivity, gas composition, and problems of energy deposition from the beam have been considered and will be reviewed briefly for convenience. The introduction of He_3^+ into the pumping sequence during the current reporting period has served to resolve the main outstanding problem of the strongly non-linear dependence of output power on pressure. The details will be discussed in Section IIIC.

Finally, during the current reporting period, quasi cw operation was achieved pointing the way toward much longer output pulses and hence, higher pulse energies. These results are discussed in Section IIID and the implications in Section IV.

A. 4278Å Performance Summary

Excitation of the charge transfer plasmas used throughout this phase of the research was produced by the APEX-I electron beam device acquired under this contract. It was constructed by Systems, Science and Software of Hayward, California and is a fast pulse, sheet beam gun emitting 100 KA pulses of 1 MeV with a 1 x 10 cm transverse cross section. As used currently, pulse shapes are nearly triangular with 20 nanosecond FWHM and optionally with a 6.6 nanosecond fall time controlled by a shorting electrode. During the experimental series reported here, the anode-cathode spacing in the output diode was increased to give a larger diode impedance and consequent peak currents between 10 and 20 KA were obtained. Larger currents were not attempted as the operation under those conditions is rendered difficult by problems of foil survivability.

The afterglow chamber used in these experiments was the ELAC-I device described previously.[23] It consisted of a laser cavity mounted to a foil support assembly and contained in a cylindrical high pressure vessel with axis of symmetry along the axis of beam propagation as shown in Figure 8.

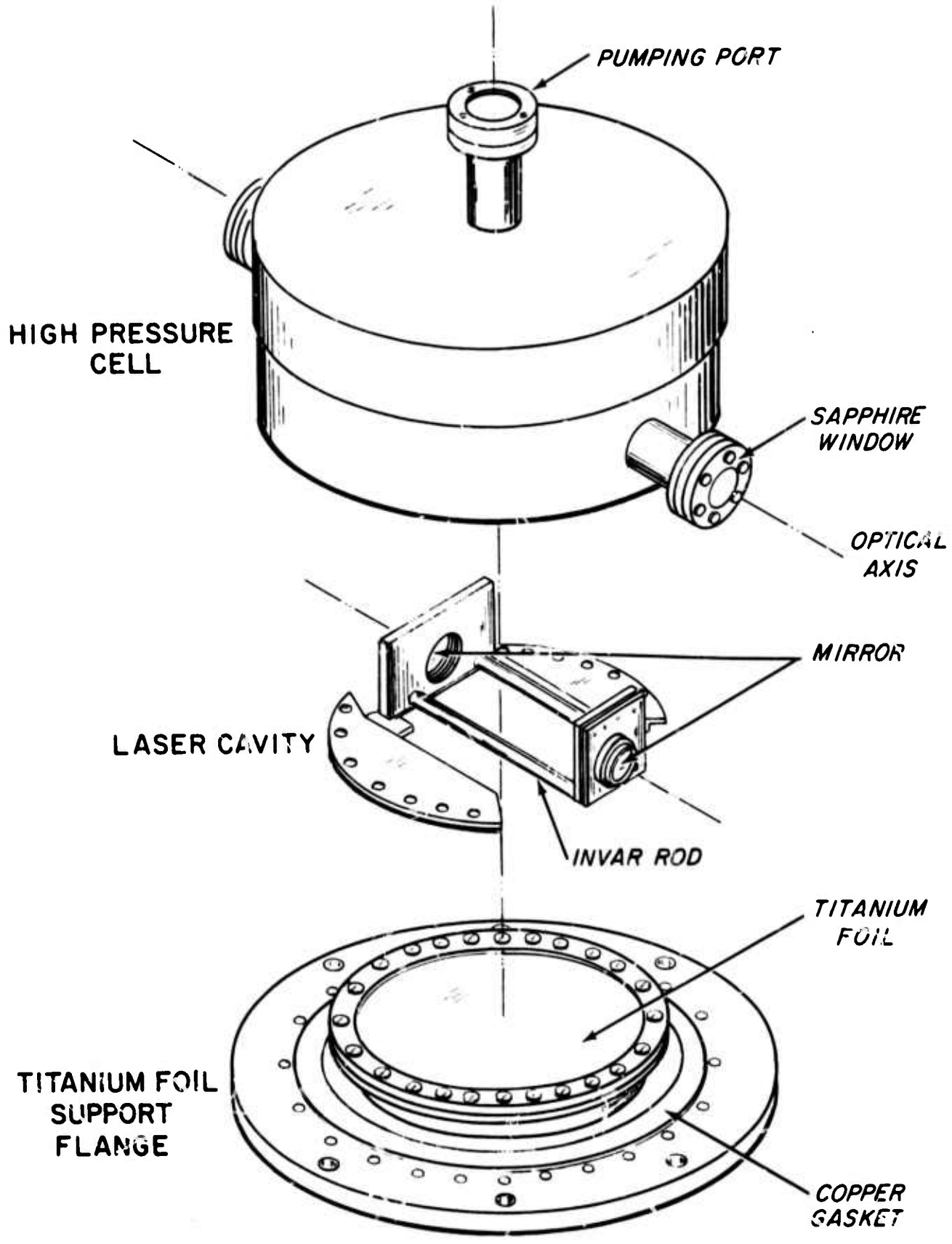

Figure 8: Exploded view of the e-beam laser afterglow chamber (ELAC-1) supporting the nitrogen ion laser work described here.

The assembly was constructed of UHV-grade stainless steel with windows and gas handling connections made with Varian-type copper shear seals. The laser cavity consisted of a pair of dielectric mirrors which were mounted to allow angular alignment, spaced with 14 cm invar rods, and contained in the pressure vessel with sapphire or quartz windows sealed across the optical axis external to the cavity as shown in Figure 8.

In operation the system was pressurized with 1 to 35 atmospheres of a mixture of helium and nitrogen. Useful partial pressures of nitrogen ranged from 2 to 120 Torr. Excitation was provided by the electron beam from APEX entering through a supported, 0.002-in. thick titanium foil window and propagating in a direction perpendicular to the optical axis. Typical operation is seen in the photograph of the laser beam propagating in a "smoky" atmosphere shown in Figure 9.

Three laser lines have been excited in mixtures of helium and nitrogen pumped by reaction set (2). Each corresponds to transitions from the same upper vibration state, v = 0, of the $B^2\Sigma_u^+$ electronic state to different lower vibration states of the $X^2\Sigma_g^+$ electronic state of the N_2^+ molecular ion. The three lines and their respective vibrational transitions are: the 3914 Å (0,0), the 4278 Å (0,1), and the 4709 Å (0,2). With the proper mirror set, each has been excited individually. The most work has been done on the (0,1) transition at 4278 Å, but since each has the same upper state, those same results should be roughly characteristic of all with the

Figure 9: Photograph recording a single 300 KW pulse from the nitrogen-ion laser. The emission consists of a single spectral line of less than 0.3 Å line-width at 4278 Å in the violet. The laser cavity is contained in the pressure vessel seen to the rear of the photograph. It is the most efficient visible, e-beam laser constructed to date, scaling at 3.0% of the energy deposited in the gas.

exception of the (0,0) transition which self-terminates at very early times.

An initial examination of the raw data relating pulse energy to e-beam deposition does not reveal a trend suggesting the nature of the dependence of output on the various diverse experimental parameters. In fact, a highly degenerate system is found for which the same output can be achieved from quite different experimental arrangements. Figure 10 illustrates this point, presenting raw data obtained with a variety of gas compositions and mirror reflectivities. Each datum has three common features, the same excitation pulse, a plane-parallel optical cavity, and the emission of the single laser line at 4278 $\overset{\circ}{A}$.

Although the plane-parallel optical cavity appeared, a priori, the most attractive in terms of analysis, in fact this is only the case for CW oscillation after stable cavity modes have developed. The transient response of such cavities to self-excitation is quite complex. This problem was considered in detail[7] during the previous reporting period and an analytical procedure was developed to describe the time-dependent growth of the plasma volume interacting with the cavity fields. A ray tracing program was written to deconvolute the time-dependent laser intensity observed for a given measured average beam divergence in order to obtain the average field-plasma interaction volume and the fraction of the energy extracted from the plasma in comparison with that "walking off" the mirrors. For example, for the data at the lower end of Figure 5, to exceed threshold, highly reflective mirrors must be used which greatly raises the ratio of

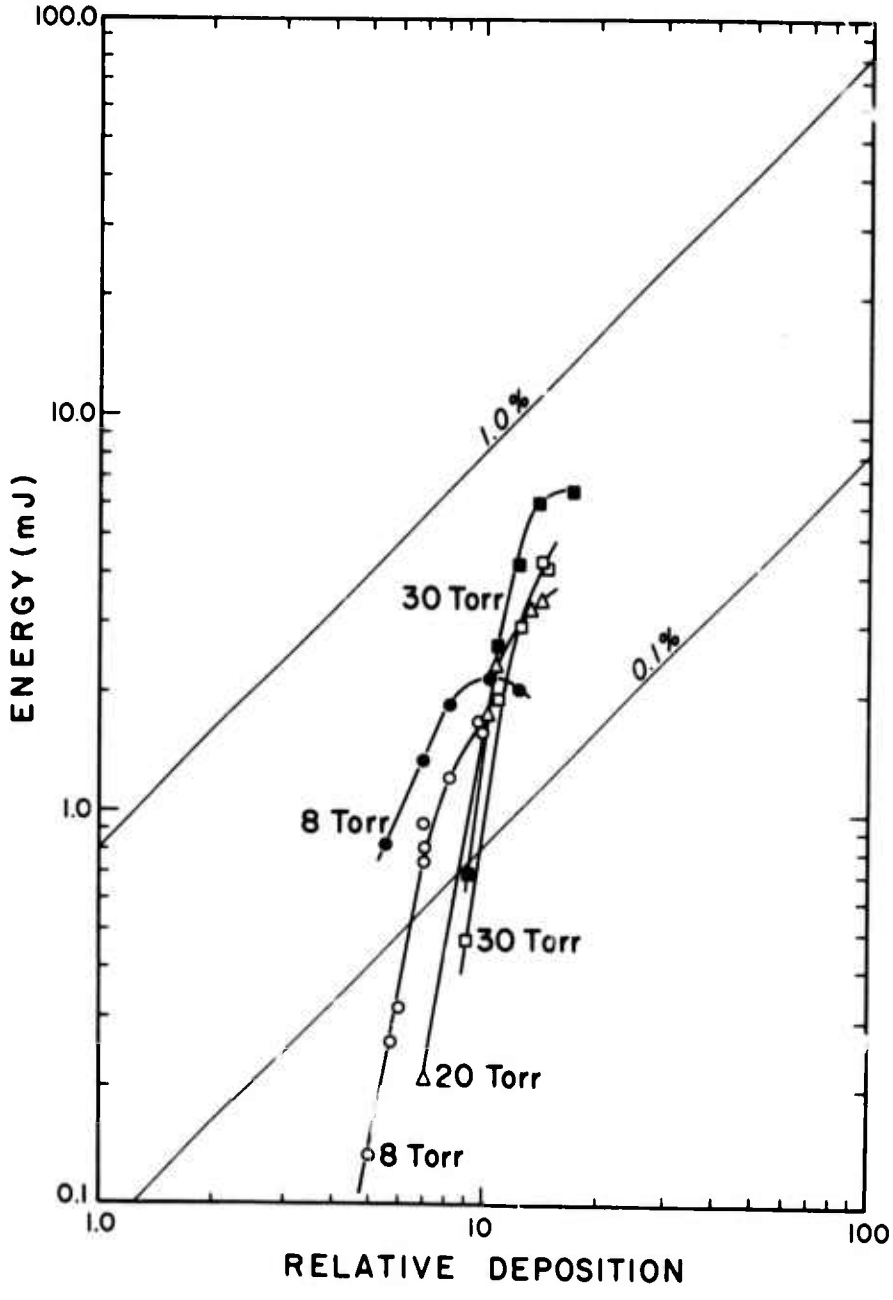

Figure 10: Summary plot of total pulse energy emitted from a 16 cm^3 volume as a function of relative deposition of energy from the electron beam. Variation of the deposition is obtained by changing the total gas pressure; hence the stopping power. The peak e-beam current is 13KA in each case. Lines of constant efficiency appear as diagonals. The partial pressure of nitrogen in Torr used in each series is shown and the difference between open and filled symbols is made by a difference in mirror characteristics.

circulating power to emitted power on any particular pass. As a result, walk-off losses are very large and in the 8% cases more energy walks-off the mirrors than is emitted.

As reported previously[7] this analysis served to show that all of the available energy was being extracted from the plasma by the fields and that the only effect of the varying mirror coefficients was to determine the rate at which that energy was extracted and whether it was routed into the transmitted beam or walked off the mirrors. This was a very important conclusion because it implied competing losses were negligible and that the energy was stored without appreciable degradation in the excited state population until stimulated to emit. Such characteristics led to the successful quasi-cw operation now reported in Section IIID.

To confirm further the concept that the total energy extracted was independent of mirror parameters, an effort was made to obtain a cavity geometry with low walk-off. Though the unfolding program is only valid for plane parallel cavities, it can be reasonably assumed that for hemispheric cavities with large angular aperture compared to the output beam divergence, ray stability exists for an appreciable region around the cavity axis. For such cavities walk-off could be expected to be negligible in comparison with plane-parallel cavities. For the same plasma conditions, then it could be expected that the energy emitted from a hemispheric cavity would roughly equal the total extracted in either and this was found to be the case experimentally. Thus, the deconvolution of the laser pulses was found to

reduce the multivariate dependence of all the data obtained to date from plane cavities to a form dependent upon a single parameter, the pressure and to yield a value in agreement with the output measured from hemispheric cavities, assumed to be lossless.

To determine the efficiency of the extraction of output energy the deposition of electron beam energy into the laser cavity must be accurately calculated. An essential factor in understanding of the energy deposition from the beam lies in the fact that scattering and stopping power do not have the same dependence on atomic number, Z^{15}. As a consequence, it is possible to have a situation in which a considerable fraction of beam energy is stopped without appreciable scattering or conversely that the scattering is so great that the simple approximation of the product of the stopping power and penetration depth seriously underestimates energy deposition, even for small fractional losses of beam energy.

The almost singular case of the light inert gases excited at beam currents below 20KA falls into the first category, and simplifying assumptions exist which render the problem tractable. Subject to limitations on the product of gas density and beam penetration depth, discussed in previous work,[7,23] the problem can be resolved into that of the differential energy loss in the gas of β-particles in a beam, the morphology of which is completely determined by the foil window through which the beam has entered. For a titanium foil, .002" thick, the following bounds on the domain of gas transparency were obtained,

$$PX\ (\text{Helium}) \leq 273\ \text{atm. cm} \qquad (26a)$$

$$PX\ (\text{Argon}) \leq 4.3\ \text{atm. cm}\ , \qquad (26b)$$

where P is the gas pressure in atmospheres and X is the penetration depth of the beam into the gas.

It can be seen from these results that, whereas the simplifying assumptions break down for argon (Z=18) at an inch of penetration at two atmospheres, they remain valid in helium (Z=2) over the entire span of parameters required for practical operation of a small test laser device. For example, at 30 atmospheres pressure, the simplified model is valid to at least 9.1 cm depth of penetration which is sufficient to describe about a half liter volume excited by a 1 x 10 cm electron beam of divergence characteristic of transmission through a .002" titanium foil window at 1 MeV for currents less than 20 KA. At higher currents, the "drag e.m.f."[24] resulting from the return currents should be considered.

A complete analysis for helium including the dependence of stopping power and foil scattering on time-dependent beam energy has been presented previously.[7,23] It has lead to an average power deposition constant of 17.3 Megawatts/ℓ/atm/KA on the leading and falling edge of the pulse and a value of 18.05 MW/ℓ/atm/KA on the plateau. However, in view of the uncertain detail of the time-dependence of the beam such analysis is excessively tedious. A re-examination of the beam scattering as evidenced by burn patterns on plastic targets has led to an equivalent but simpler expression for the

average power disposition of

$$17.2 \text{ Megawatts}/\ell/\text{atm}/\text{KA} \quad , \tag{27}$$

on the beam axis at the depth of penetration of the cavity center. This value was used for the calculation of efficiencies throughout the remainder of the work reported here.

The actual values of current density in the electron beam were measured with a calibrated Faraday cup which replaced the pressure vessel and laser cavity. Particular attention was paid to relative timing and cable lengths so that the temporal relation between beam current and laser output could be determined subsequently. Output from the Faraday cup was directly recorded with a 519 oscilloscope. Laser performance data has now been collected over a broad span of experimental parameters. Total pressures have ranged from 1 to 35 atmospheres with partial pressures of nitrogen varying from 2 to 120 Torr. As discussed immediately above, the variation of cavity constants affected the rate of energy extraction from the e-beam plasma, but had little effect on its total. To within rather unrestrictive limits the deconvolution program was able to reduce the parameterization of the laser performance to dependence upon a single variable, the total pressure. The limits bounding this parameterization are primarily a consequence of two effects.

1) If the ratio of nitrogen to helium exceeds the limits inferred in Table 4, laser output will be drastically reduced or prevented altogether.

2) If the combination of mirror loss and gas composition is such as to delay the onset of lasing until beam current is beginning to decrease at the end of the e-beam pulse, outputs will again be reduced or terminated. Evidently, in this case, the excited state chemistry is altered by the termination of the beam and competing processes such as recombination with the cooling electrons become important.

Except for data obtained under those conditions, most of the data could be reconciled with a very simple parameterization of the total energy extracted from some standard plasma volume.

The largest laser outputs found at 4278Å in the raw data were from the hemispheric cavity having 27% transparency and the average volume appropriate to that data was 16.2 cm^3. This was chosen as the "standard volume." Since walk-off was assumed zero for the hemispheric cavities, the largest laser outputs (from the 20 - 35 atm. data) simply correspond to unscaled measurements of the total energy emitted into the laser output beam. For the purposes of parameterization, other measurements were scaled to obtain the total energy extracted from a 16.2 cm^3 volume of the plasma, so that

$$E_x = (1 + \bar{W}) \times (16.2/\bar{V}) \times E_e \quad , \qquad (28)$$

where E_e is the energy emitted by the cavity into the laser beam, E_x is the total energy extracted from the plasma by the fields, $\bar{V}$ is the average volume from which it was extracted, and $\bar{W}$, the average ratio of energy walking-off the mirrors to that emitted into the beam. As mentioned above, for hemispheric cavities, $\bar{W}$ was assumed to be zero.

The resulting summary of measurements is presented in Figure 11. The total energy extracted from the 16.2 cm^3 of the charge transfer plasma is plotted as a function of total gas pressure. Data all corresponds to excitation at the level of 76 mJ/atm by a standard discharge pulse containing 275 μ coul of integrated current. The partial pressures of nitrogen varied from 2 to 120 Torr and are indicated by the type of symbol plotted. Shown for comparison are the theoretical results obtained in the previous section by assuming, 1) that the inversion is pumped primarily by He_3^+, 2) that reaction (25) is sufficiently fast that the concentration of He_3^+ is in thermal equilibrium with the He_2^+ after a few nanoseconds as described in (26) and 3) that one photon per He_3^+ is ultimately extracted by the fields in the laser cavity. It can be seen that the expected laser output is in excellent agreement with the reported data shown in Figure 11. The 47°C temperature corresponds to the value reasonably expected in a helium sample, initially at room temperature, heated by a 20-30 nsec. 1 MeV electron beam pulse of 275 μ coulomb. If this agreement, in fact, represents confirmation of the validity of the kinetic model summarized in (2), then the

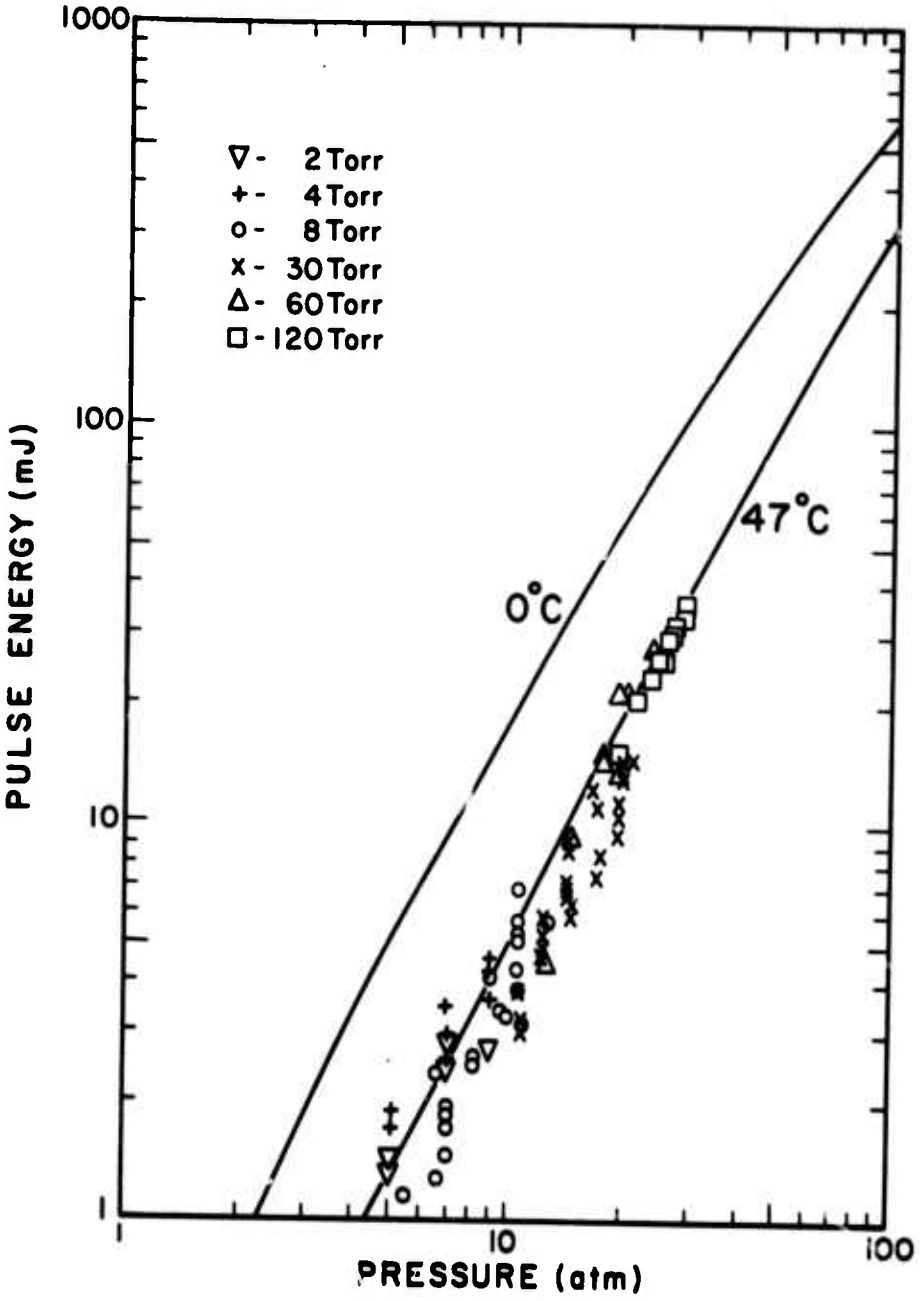

Figure 11: Summary plot of total laser pulse energy emitted from a 16 cm^3 volume as a function of total gas pressure. The integrated e-beam current corresponds to 275 μ coulomb for each case. Data points represent output at 4278 Å and different partial pressures of N_2 are indicated by the shape of the data point as follows, except for + and ▽; 0 - 8 Torr, X - 30 Torr, Δ - 60 Torr, □ - 120 Torr. The + and ▽ symbols plot the total pulse energy extracted at 3914 Å from the plasma at 4 and 2 Torr, respectively by the fields in the cavity and has been corrected for reabsorption at the end of the pulse. Solid curves plot theoretical predictions of the kinetic model described by eqns. (2a) - (2e) for the average gas temperatures indicated.

strong increase in laser power and efficiency observed at increasing pressures should be even more readily achieved through a reduction of the gas temperature. Expected outputs for $0^{o}C$ are also shown in Figure 11.

The dependence found for the output pulse energy on e-beam current, however, was much less than linear and showed a type of saturation between 15 and 25KA which made analysis in terms of time integrated current more attractive. Figure 12 shows this dependence of pulse energy, parametrically on peak electron beam current. The time-dependent electron beam currents recorded by the Faraday cup and corresponding to each of the nominal values appearing in Figure 12 are shown in Figure 13. Since the locii of constant efficiency on an output plot such as that of Figure 12 are different for each excitation current, comparisons of efficiency are facilitated by the normalization of the data to some standard value of excitation. Further extraneous dependence on the time of onset of threshold and the time at which the diode is shorted in the case of supplementary "clipping" can be removed by normalizing to a standard value of time-integrated beam charge passed through the plasma prior to the time the laser power falls to 1/e of its peak value. Thus the values of output summarized in Figure 13 were individually normalized to the energy which would have resulted from discharge of only 275 μ coulomb of beam current prior to the 1/e time on the trailing edge of the laser pulse. There is little resulting change in the data as seen in Figure 14 other than the fact that they are now directly comparable to the same locii of constant efficiency. The lines representing constant

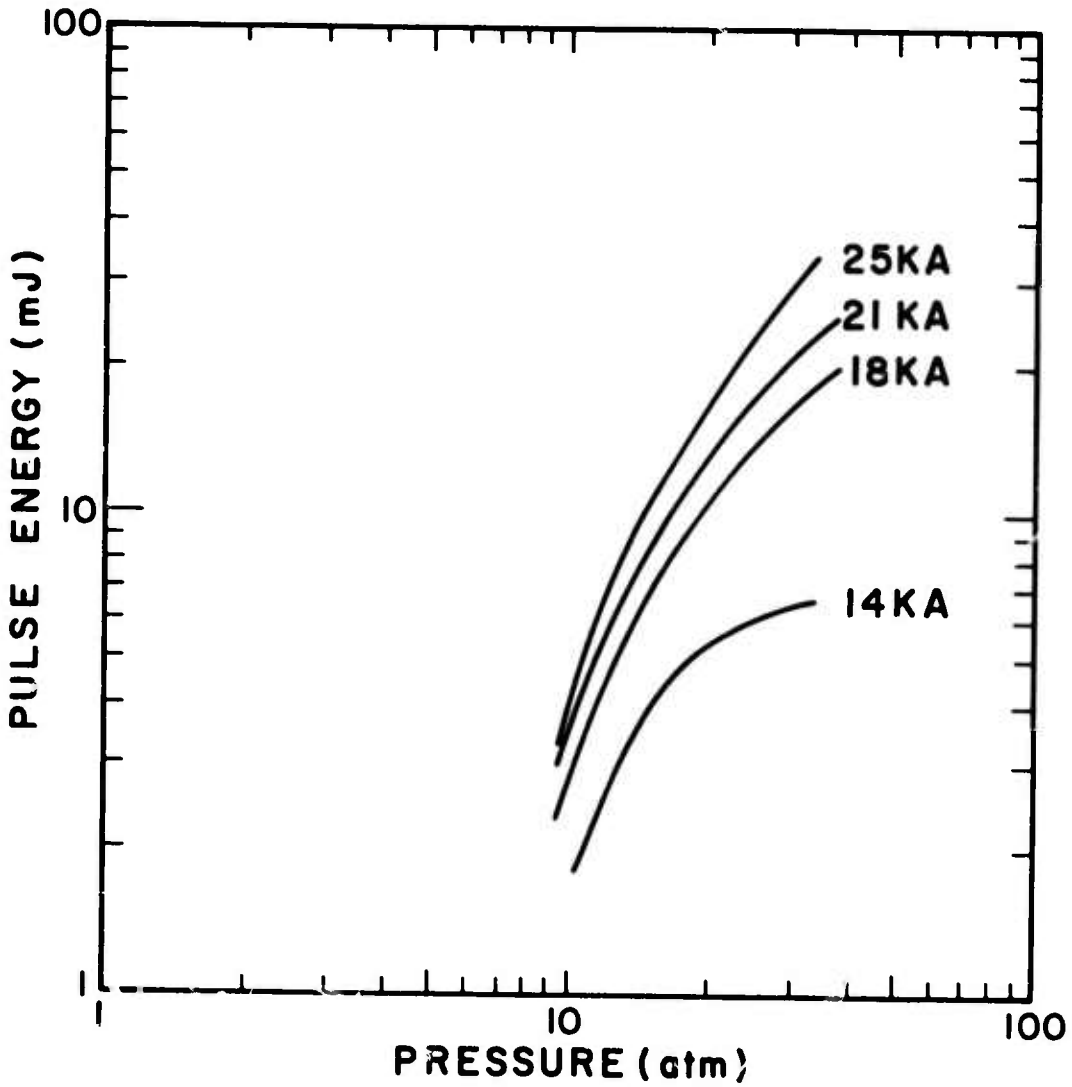

Figure 12: Summary plots of the total laser pulse energy emitted at 4278 Å from a 16 cm^3 volume as a function of total gas pressure for the several indicated values of the nominal electron beam currents shown in Figure 13.

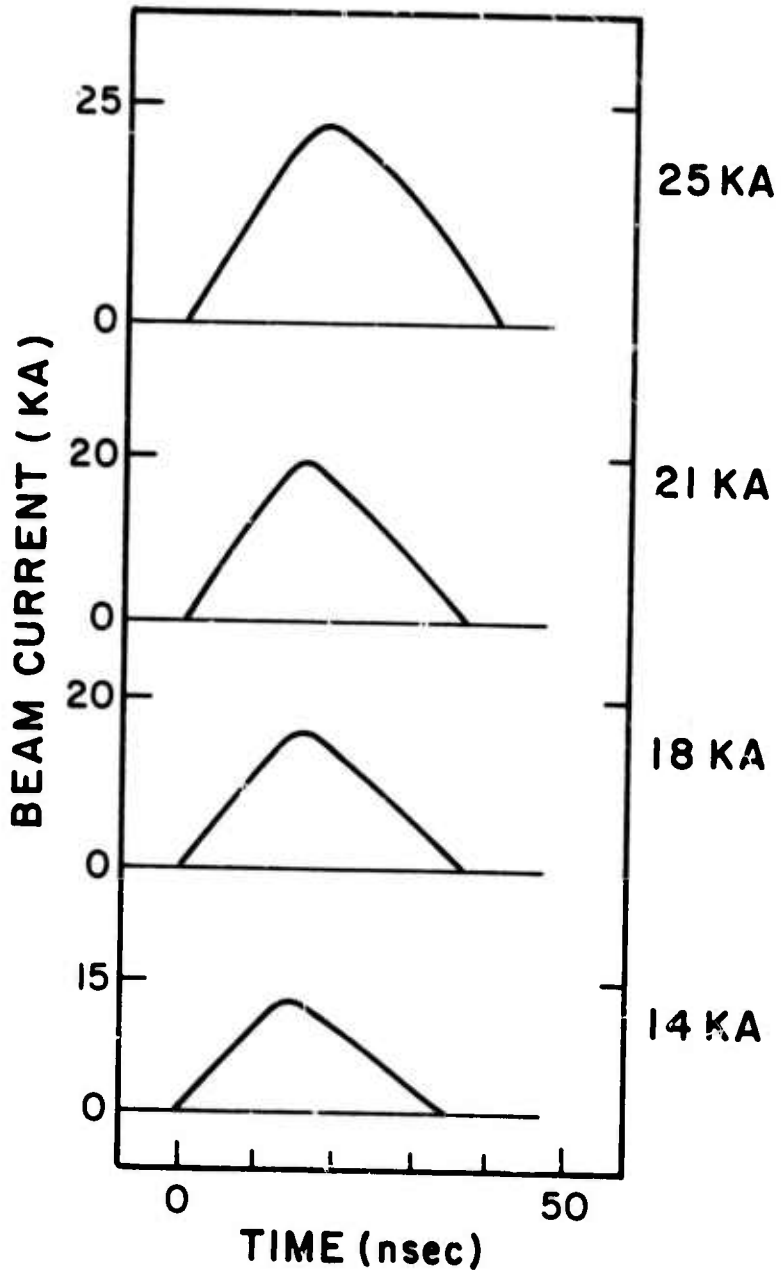

Figure 13: Recordings from a 519 oscilloscope of the time-dependence of the electron beam current for the nominal values of current for which the data of Figure 12 was obtained.

efficiency of output referred to the energy deposited in the lasing volume by 275 μ coul. of e-beam discharge are shown for comparison. It should be noticed that the performance for one additional discharge condition has been added, namely, that for separation of the laser cell and e-beam gun by a 30 cm drift space to facilitate subsequent thermal scaling of the laser.

None of the current-dependent data has been de-convoluted and the pronounced "droop" at the higher pressures is most probably due to the excessively late onset of the lasing threshold. Most generally, when corrected and normalized to 275 μ coul. of beam charge, the data groups around the theoretical model as shown in Figure 11. Earlier attempts[7] to empirically fit the data had noted it grouped more closely around a line of slope 2.2. Since the energy input deposited by the beam varied linearly with pressure, the consequent efficiency of energy extraction could be modeled to vary with the 1.2 power of the pressure. An extrapolation of the fit to the data appeared to intersect the theoretical limit around 100 atm. so that the efficiency was conveniently expressed as

$$E = 6.5\% \ (P/100)^{1.2} \quad . \qquad (29)$$

The best output at room temperature was found to be 36 mJ at 28.7 atm which corresponded to an efficiency of 1.6%.

B. Other Transitions, 3914Å and 4709Å -

As mentioned previously[7,8] the Franck-Condon factors for the (0,0) and (0,2) transitions between the same electronic states are sufficiently

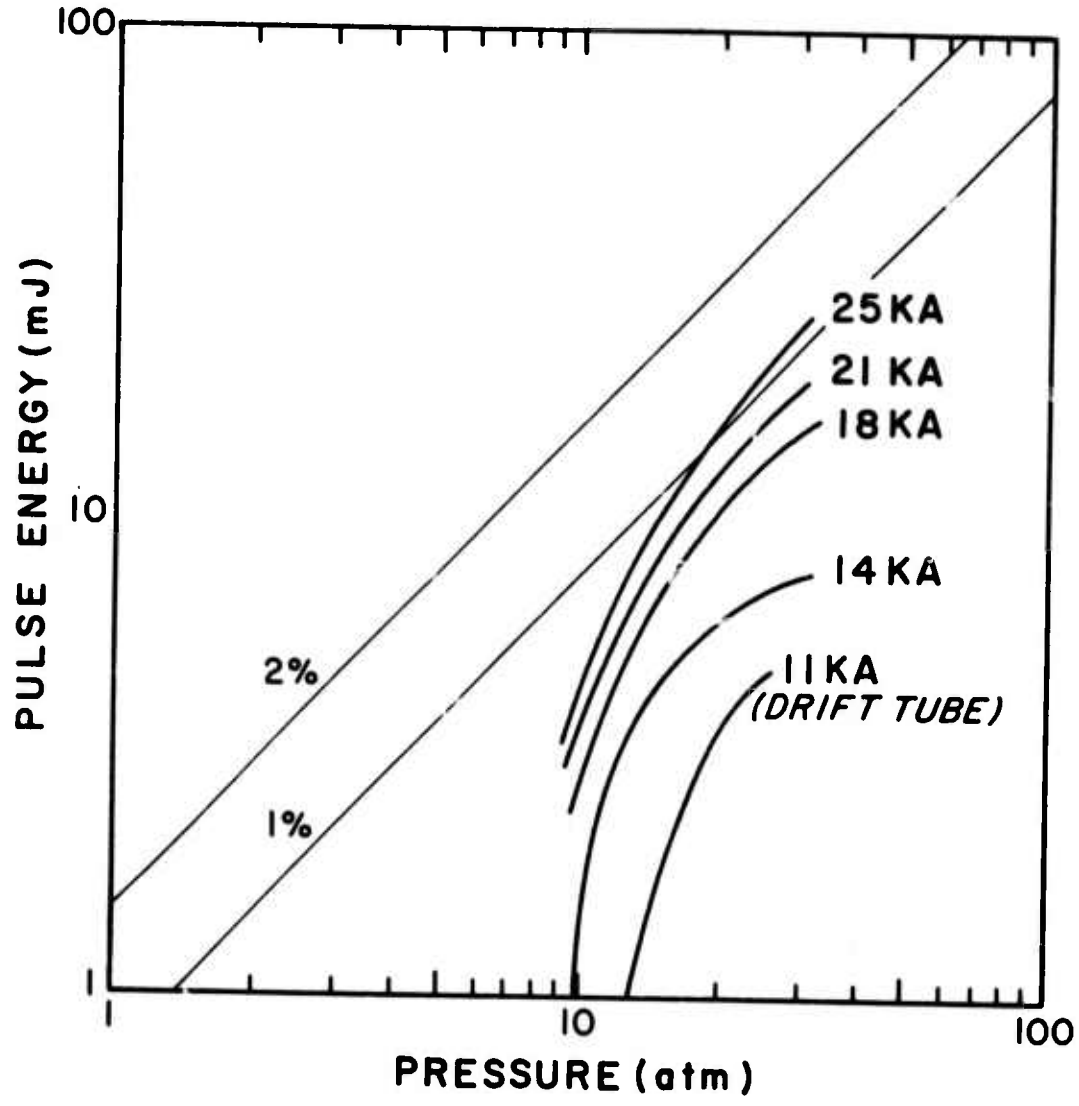

Figure 14: Summary plot of the equivalent laser pulse energy emitted at 4278 Å from a 16 cm^3 volume for 275 μ coulomb of e-beam charge. Data for the several different nominal discharge currents indicated are shown.

favorable that the threshold should be attained with the proper mirror sets. This was observed to be the case[7,8] and each transition could be individually excited with the proper choice of mirrors. Figure 15 shows typical laser outputs in comparison with the (0,1) transition at 4278 Å. As would be expected, a priori from the 2.3:4.4:1 ratio for the Franck-Condon factors from the upper v'=0 level of the $B^2\Sigma_u$ state to the lower v"=0,1, and 2 levels of the $X^2\Sigma_g$ the onset of threshold was proportionally delayed.

As can be seen, the 3914 Å component self-terminates in about 2 nanoseconds and gives a measure of the time required for the lower laser state to "fill". Since the lower state of the 4278 Å differs only in vibrational quantum number, it has the same degeneracy and should "fill" to terminate the 4278 Å transition in a comparable time. That it does not, as seen in the figure, is strong evidence for the existence of an unblocking process tending to quench the vibrational excitation of the lower, v"=1, state of 4278 Å transition. How this process leads to quasi-cw operation will be discussed in Section IIID.

The problem of determining the absolute energy deposition from the electron beam in the radiating volume are particularly acute in the case of the 3914 Å emission. Since the laser output in this case occurs so early in the course of the e-beam pulse, it is misleading to correlate the laser pulse energy with the entire e-beam input energy. Clearly it is only the e-beam energy which is deposited before the termination of the laser pulse that can contribute to the laser excitation. As in the case of the current-

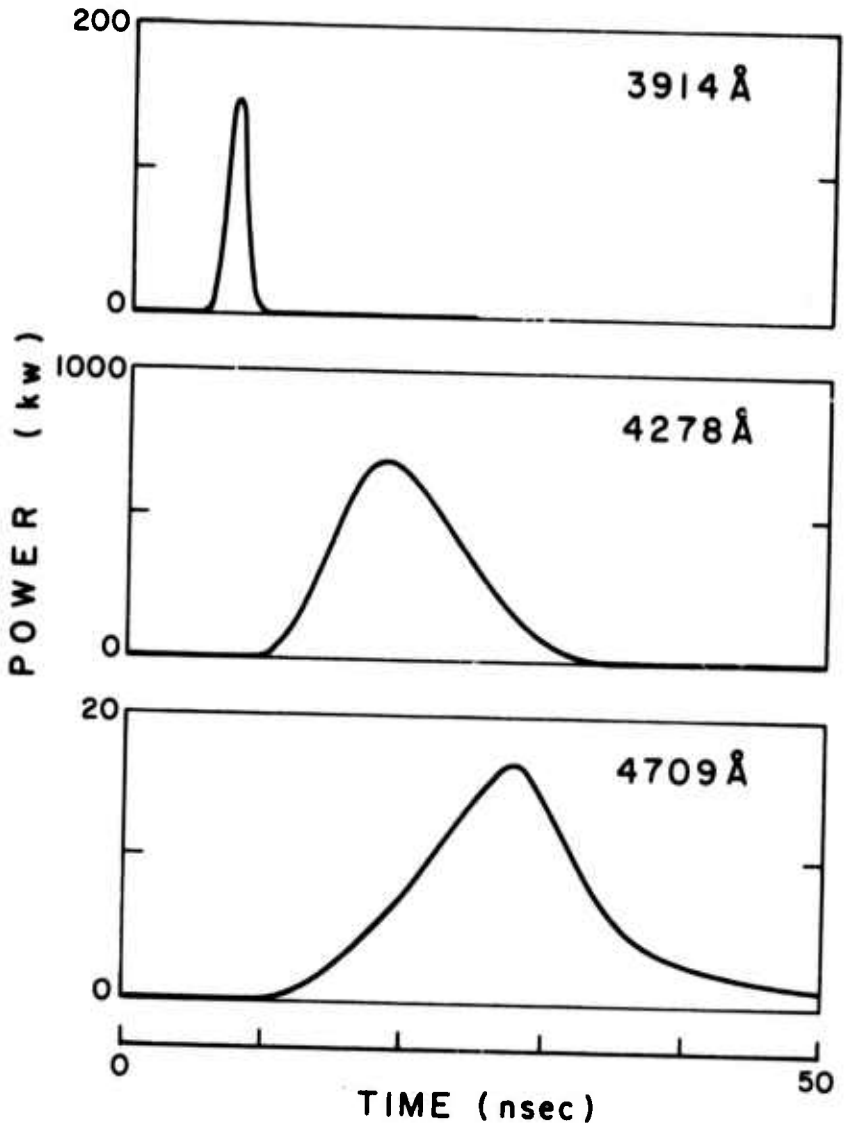

Figure 15: Time-resolved power measurements of the nitrogen ion laser outputs for three different mirror sets individually optimizing the (0,0), (0,1), and (0,2) transitions at 3914, 4278, and 4709 Å, respectively. Corresponding total pressures are, from top to bottom, 10.8, 14.9, and 16.3 atm. The time scale is indicated and has been shifted so that the zero corresponds to the beginning of the e-beam current output.

dependent data, in the case of the 3914 Å output the procedure was adopted of considering only that fraction of the e-beam energy input prior to the termination of the laser output pulse.

Because of the drastic difference in the pulse shape of the 3914 Å transition the growth of the interaction volume[7] in the laser cavity was quite different as evidenced by the considerably increased divergence of the output beam. This, consequently, offered the best test of the deconvolution procedure because variance of divergence and interaction volume had been relatively small in the case of the (0,1) transition at 4278 Å. For the self-terminating (0,0) transition at 3914 Å average interaction volumes were found to vary from 3.4 to 14 cm^3 which was sufficient to more than mask other systematic variation of laser output with experimental parameters such as pressure and current. Figure 16 shows the almost random appearance of the performance data for the 3914 Å output energy plotted in the lower half of the graph. The marked improvement obtained in the upper half was the result of the deconvolution analysis, particularly the removal of the dependence on interaction volume. All data are represented in the upper half and the shading of the points to indicate the beam current has been removed to reduce confusion. Whereas the organization of the data into a compact group is the result of scaling the interaction volume, the large displacement of the points upward is the result of correcting for absorption and walk-off.

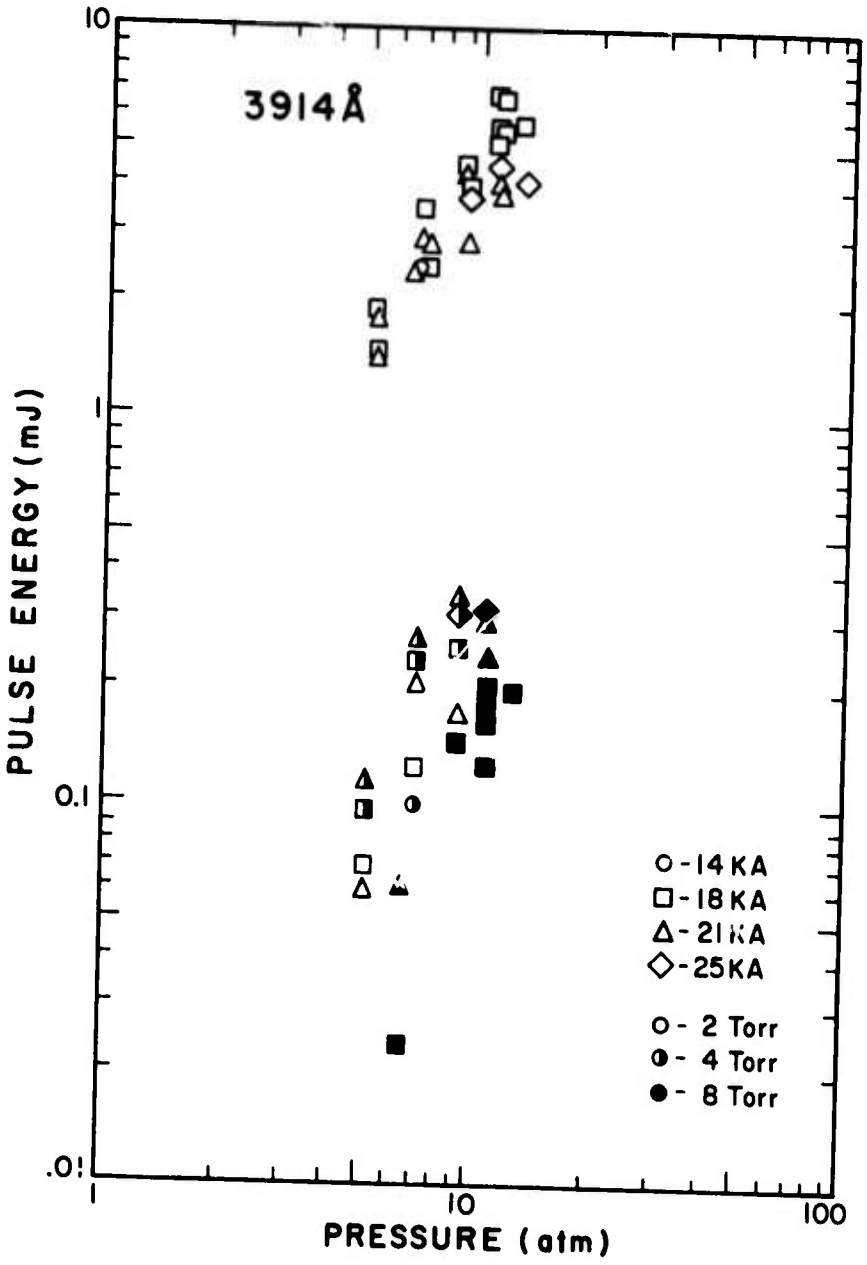

Figure 16: Summary plot of laser pulse energy at 3914 Å as a function of pressure. Data in the upper portion of the graph show the gross energy extracted from the plasmas by the circulating power in the cavity, normalized to a volume of 16.2 cm^3 and a beam discharge of 275 μ coul. Much of the energy is reabsorbed with only the net energy plotted in the lower half of the graph being detected in the output-beam of the laser. In each case the shape of the data point gives the nominal beam current and for the net energy data the partial pressure of nitrogen is given by the shading of the symbol.

Because of the drastic difference in the pulse shape of the 3914 Å output two expressions for the energy extracted were necessarily considered. First was the net energy extracted from the plasma, which is the measured output emitted into the beam corrected for walk-off losses according to equation (28). For this case these losses were comparable to those observed for the 4278 Å data at comparably low pressures. Second, however, was the gross energy extracted. This was the net energy plus the energy extracted by the fields in the cavity and subsequently re-absorbed at the end of the laser pulse. This re-absorption loss is also calculated by the unfolding program and in the case of the data of Figure 16 was quite significant. This is again in contrast to the 4278 Å data for which re-absorption was always less than 7% of the output and, hence, was neglected. This correction for re-absorption is the largest contribution to the upward displacement of the data seen in Figure 16 and requires that the data of the upper half of the graph be considered the gross energy extracted from the plasma by the fields in the cavity. When plotted on the "master curve" of laser performance, as shown in Figure 11, the data of the gross extraction at 3914 Å "fit" smoothly both the theory and experimental data for output at 4278 Å.

These results on other transitions in the helium-nitrogen laser support three important conclusions. First is that the deconvolution procedure

is realistic and defensible and thus that the energy available for extraction by the fields can be represented by a simple "master performance curve" as seen in Figure 11. Second is that since threshold is indeed achieved for the (0,0) component of the B → X electronic transition, the branching ratio of the output channels of the pumping reaction (21) strongly favors the upper B state and hence branching in the output channels poses no obstacle to the extraction of one photon per He_3^+ ion. Finally, the third point is that the energy pumped into the B state of N_2^+ is effectively stored until the fields resulting from the spontaneous emission build up enough to start the stimulated emission ultimately extracting the energy stored in the inversion. Even though the 3914 and 4278 Å outputs start at substantially different times in the life of the plasma, the same integrated extraction efficiency is achieved. That this energy is not extracted in the (0,2) transition at 4709 Å is a consequence of the relatively small transition porbability and hence slow accumulation of spontaneous emission at this wavelength necessary to initially excite the cavity oscillations. Evidentally the cooling of the plasma at the end of the e-beam discharge destroys the stored energy by recombination. Either a longer duration e-beam pulse of an external source of cavity excitation would be necessary to extract the stored energy at 4709 Å.

C. Thermal Enhancement of the Reaction Sequence -

As discussed in the theory of Section II, the low dissociation energy of He_3^+ makes a thermal equilibrium of He_2^+ and He_3^+ populations likely. It was shown in Figure 11 that the assumption of such an equilibrium correctly explains the observed data if one photon is being extracted for each He_3^+ ion present. The equilibrium ratio given in (26) is even more sensitive to gas temperature than pressure and suggests that the theoretical limit of 10.5% efficiency may be approached through thermal enhancement of the population of He_3^+.

Unfortunately the existing laser device ELAC-1 was not designed for thermal cycling and this together with the relatively high thermal conductivity of helium made the accurate control of gas temperature very difficult. Best control was obtained by mounting ELAC-1 on a 30 cm drift tube which was then connected to the electron beam gun with an additional foil assembly. When the drift tube was filled to a rather critically defined pressure of nitrogen ($\sim$ 500μ) about half the electron beam current could be conducted to the laser device. Under these conditions the more limited thermal conductivity reduced the constant thermal flow from the gun and afforded some control over temperature in the laser.

Cooling was accomplished by circulating cold liquid nitrogen vapor through a heat exchanger attached to the pressure vessel containing the laser device and the average gas temperature in the cell was obtained by measuring

the pressure as the system cooled. Since the laser cavity was positioned closest to the source of the thermal flow into the heat exchanger, the actual temperature in the laser cavity was necessarily higher than the average gas temperature. Hence, the following data presented underestimates the effect on laser output of reduced gas temperatures by underestimating those temperatures.

The performance plot shown in Figure 17 illustrates the substantial improvement in output pulse energy obtained for a 40°C decrease in average gas temperature. For comparison room temperature values are shown and it can be seen that both output and efficiency achieved with only the attenuated beam available from the drift tube exceeded anything previously obtained at room temperature even at the most optimal values of current and pressure.

Although the actual value of temperature in the laser cavity remained obscure the variation of laser output with changes in average gas temperature in the pressure vessel could be obtained. Figure 18 shows the effect of continuously cooling the gas prior to the election beam discharge at a nominal current down the drift tube of 11KA. As can be seen factors of improvement of as large as 10 were achieved for a 42°C decrease in average gas temperature. As would be expected from the expression for the equilibrium constant, the limiting temperature appears not to have been reached at -20°C.

In an attempt to verify that the thermal enhancement observed was not limited to excitation at the low current available from the drift tube,

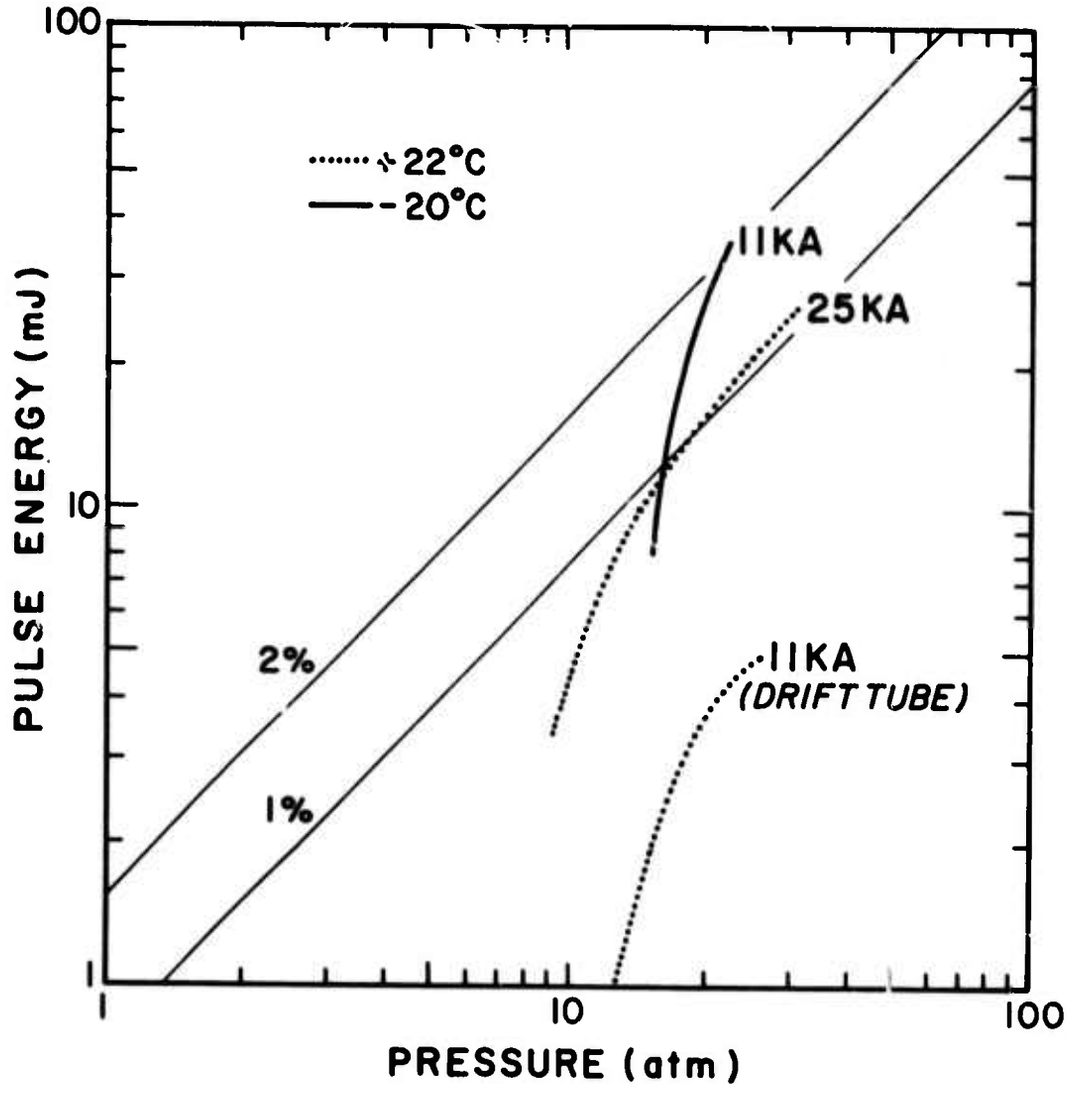

Figure 17: Performance plot of the thermal enhancement of the total laser pulse energy emitted at 4278 Å as a function of total gas pressure for 275 μ coul. of e-beam discharge into 16 cm^3. Dashed curves reproduce the room temperature curves of Figure 14 for the nominal currents indicated and the solid curve plots data obtained at an average gas temperature of -20°C for the current shown.

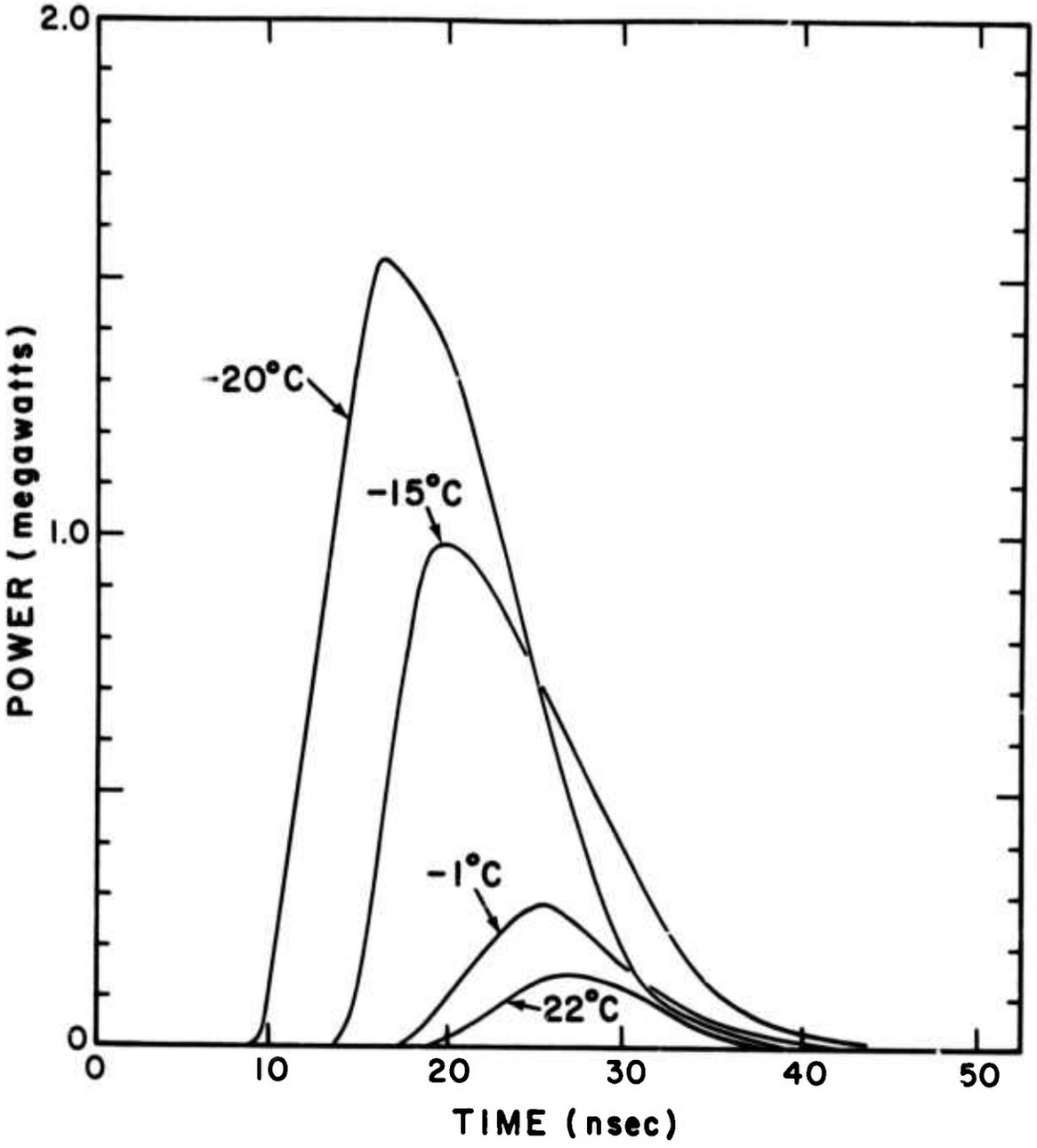

Figure 18: Thermal scaling of the helium-nitrogen charge transfer laser. Plotted parametrically as a function of gas temperature are time resolved power measurements of the violet line at 4278 Å. Data are shown for the discharge of 190 μ coulomb into 21 atm. pressure of helium containing 60 Torr of nitrogen. The time scale has been normalized so that the zero corresponds to the beginning of the e-beam current output.

the laser device and liquid N_2 heat exchanger were connected directly to the electron beam gun. Though not as remarkable as the effects on the outputs from the drift tube configuration shown in the previous figure, the effects of a similar decrease in average temperature on discharges at higher currents and pressures were substantial. "Best" outputs at each pressure were increased by a factor of approximately 2 for a 40 to 50°C decrease in the average gas temperature which in this configuration even more seriously underestimated the actual gas temperature in the laser cavity.

Figure 19 plots the performance data obtained at the higher beam currents available in the closely coupled gun-laser configuration for a -20°C average temperature. For comparison the locus of the room temperature data given by (29) is shown as a solid curve. The new data appears to be arranged parallel to the room temperature locus and as such could be parameterized in an analogous manner by the following empirical expression for the efficiency over the 10 - 35 atm pressure range examined,

$$\varepsilon(-20°C) = 10.5\%(P/80)^{1.2} \quad , \qquad (30)$$

where P is the equivalent gas pressure at room temperature, as in the expression for the efficiency at room temperature, eq. (29) and 10.5% is the revised theoretical limit on efficiency.

At the -20°C average gas temperature in the closely coupled configuration a peak power of 5.2 Megawatts at 4278 Å has been obtained at an average gas density corresponding to a pressure of 35 atmospheres at room

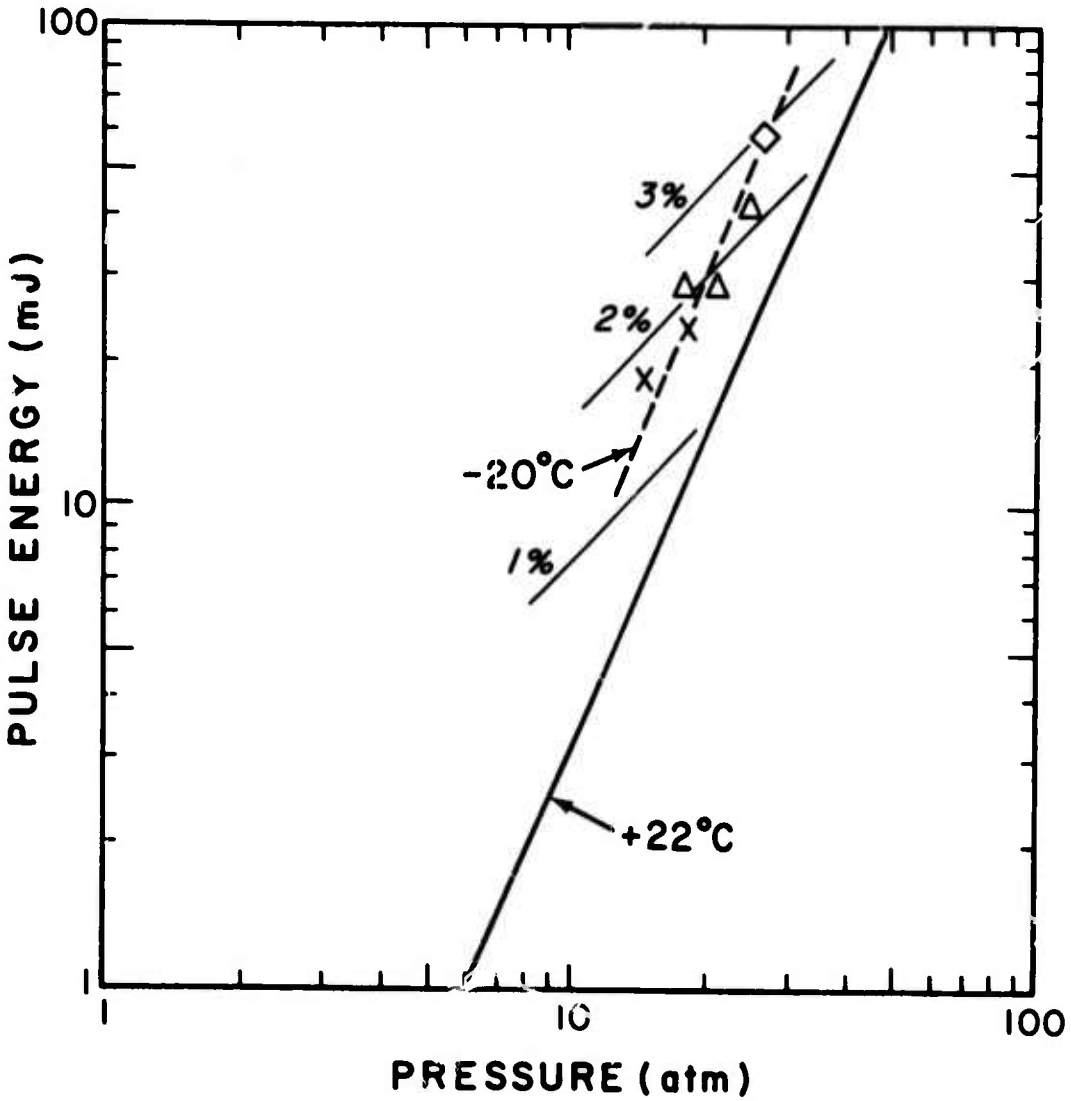

Figure 19: Performance plot as a function of total gas pressure of the thermal enhancement for the laser pulse energy emitted at 4278 Å for 275 μ coul. of e-beam discharge into 16 cm^3 of gas initially at -20°C "average" temperature. The shape of the data points give the partial pressure of nitrogen to be: 30 Torr (X), 60 Torr (Δ) or 90 Torr (◇). The locus of the corresponding room temperature data given by eq. (29) is shown as a solid curve. Lines of constant efficiency are shown for efficiencies indicated.

temperature. The corresponding pulse energy was 80mJ and represented an output efficiency of 3% relative to the energy deposited by the electron beam. This is a peak density of

$$P = 320 \text{ Megawatts/liter} \tag{30a}$$

$$E = 5 \text{ Joules/liter} \tag{30b}$$

at an efficiency,

$$\varepsilon = 3\% \quad . \tag{30c}$$

It can be reasonably expected that further thermal enhancement will raise these levels even closer to theoretical limits.

D. Quasi-cw Operation -

An additional benefit accrued during the operation at lower temperature in that quasi - cw operation of the laser was achieved at 4278 $\overset{\circ}{A}$. Output power was found to accurately follow input power after onset of threshold. Data shown in Figure 20 is typical of the close correlation of output power with a constant percentage of power input to the lasing volume, in this case at the 3% level. Such operation is of extreme importance as it points the way toward much longer output pulses to be obtained from longer discharge pulses.

This operation is believed to be the result of the quenching of the vibration of the population of the lower laser level by the electron

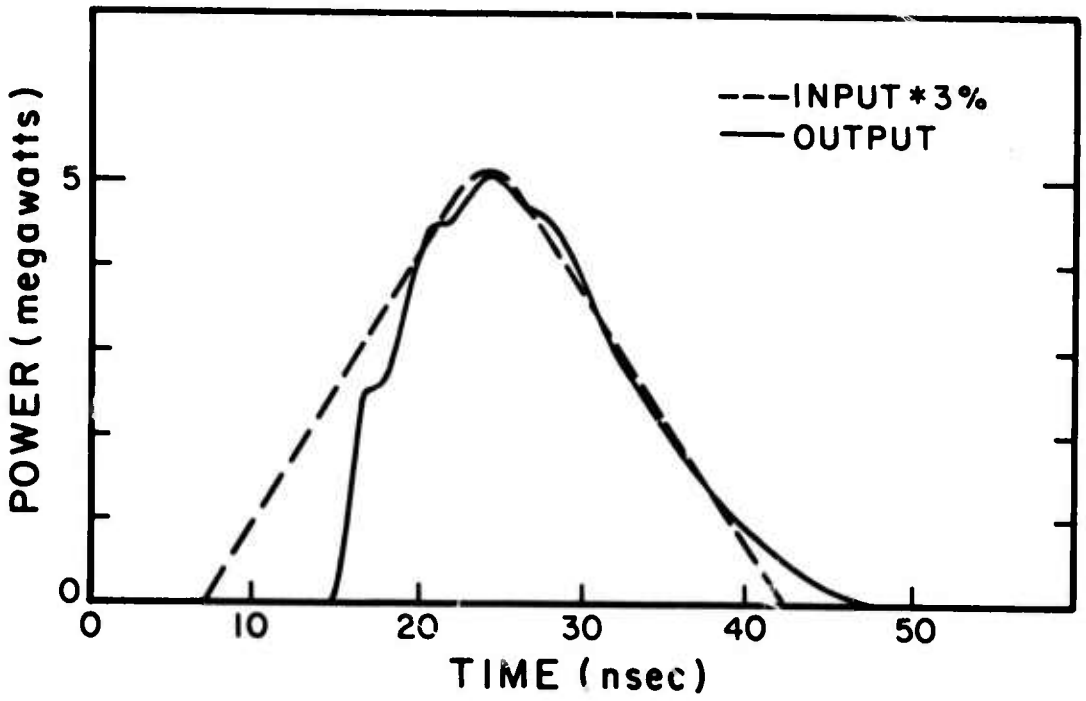

Figure 20: Plot of data showing quasi-cw operation of the helium-nitrogen laser. The solid curve shows output power at 4278 Å emitted from an electron beam discharge into 35 atmospheres pressure of helium containing 120 Torr of nitrogen. The dashed curve shows 3% of the corresponding power deposited in the laser cavity.

capture-autoionization sequence

$$N_2^+(X^2\Sigma_g)_{v=1} + e \rightarrow N_2^{**}{}_{v=1} \qquad (31a)$$

$$N_2^{**}{}_{v=1} \rightarrow N_2^+(X^2\Sigma_g)_{v=0} + e \qquad (31b)$$

where the double asterisk indicates an autoionizing state. This would be the analog for molecular ions of the rapid resonant attachment - detachment process by which free electrons transfer vibrational energy to or from neutral molecules.

Reaction set (31) in effect transforms the helium-nitrogen kinetic system into a true 4-level laser and offers the future possibility of very long output pulses or even cw operation at relatively high saturation levels.

IV IMPLICATIONS

In summary it appears that the kinetic sequence pumping the helium-nitrogen charge transfer laser must be structured as follows:

$$He^+ + 2He \rightarrow He_2^+ + He$$

$$He_2^+ + 2He \rightleftarrows He_3^+ + He$$

$$He_3^+ + N_2 \rightarrow N_2^+(B^2\Sigma_u) + 3He$$

$$N_2^+(B^2\Sigma_u) + h\nu \rightarrow N_2^+(X^2\Sigma_g) + 2H\nu \quad .$$

The excellent agreement obtained between the room temperature measurements and the predictions of this model with the assumption of one photon per He_3^+ ion appears to confirm the utility of this representation of the reaction sequence. It is not only able to explain the strongly non-linear dependence on gas pressure of the energy of the output pulse of the laser, but has also succeeded in predicting a strong inverse dependence on gas temperature, subsequently confirmed by the work reported in detail in Section IIIC. It is, then consistent with this model to expect that the proper choice of temperature and pressure will favorably adjust the equilibrium ratio of He_3^+ to He_2^+ so that the theoretical efficiency of 6 to 10% for the helium-nitrogen charge transfer laser can be closely approached.

More immediate implications concern the further thermal scaling of the current nitrogen charge-transfer laser. It now appears that the theoretical efficiency of 10.5% for the 4278 $\mathring{A}$ transition will be attained at

operating pressures around 40 atm at sufficiently low temperatures. Even at the relatively low operating charges of 275 μ coul currently used, this will yield an output of 20 J/liter. A value of 5 J/liter has already been attained. Since quasi-cw operation has been achieved an increase in e-beam pulse duration from a nominal 20 nsec to 100 nsec should bring the value projected at 40 atm to 100 J/liter. Funds to support procurement of a longer pulse-forming line for APEX have been requested in order to verify this projection.

Since operation at longer pulse lengths is expected to prove successful a visible laser of exceptionally high average power could be pumped by charge transfer if development along those lines appeared warranted. It can be expected that some type of sustainer excitation could be arranged to pump of the order of 10 liters at the 3000 μ coul/pulse level with a repetition rate of 100 pps. Then, at 40 atmospheres pressure a laser with 200 KW average power at 4278 Å could be realized at projected levels of efficiency.

While such projections are, of course, speculative, these are the implications of the recent successes with the thermal scaling of the nitrogen ion laser discussed in this report. While it should be realized that the nitrogen ion laser is only the first example of the new class of e-beam charge-transfer lasers,[9] and that other similar systems offer the possibilities of even higher efficiencies and broader selections of output wavelengths, these results observed for the emission of 4278 Å laser radiation point to the nitrogen ion laser as a device of considerable significance and clearly confirm the importance of charge transfer reactions as laser pumping mechanisms.

REFERENCES

1. D. R. Bates, A. E. Kingston, and R. W. P. McWhirter, Proc. Roy. Soc. (London) A267, 297 (1962).

2. D. R. Bates and S. P. Khare, Proc. Phys. Soc. (London) 85, 231 (1965).

3. C. B. Collins, Phys. Rev. 177, 254 (1969).

4. C. B. Collins, Phys. Rev. 186, 113 (1969).

5. R. Deloche, P. Monchicourt, M. Cheret, and F. Lambert, Phys. Rev. A, (to be published).

6. C. B. Collins, J. M. Carroll, F. W. Lee, and A. J. Cunningham, (submitted to Appl. Phys. Lett.)

7. C. B. Collins and A. J. Cunningham, Sixth Semi-Annual Technical Report No. UTDP ML-03, Contract No. N00014-67-A-0310-0007, The University of Texas at Dallas (March 1975).

8. C. B. Collins and A. J. Cunningham, Appl. Phys. Lett. 27, 127 (1975).

9. C. B. Collins, A. J. Cunningham, S. M. Curry, B. W. Johnson, and M. Stockton, Appl. Phys. Lett. 24, 477 (1974).

10. C. B. Collins, A. J. Cunningham, and M. Stockton, Appl. Phys. Lett. 25, 344 (1974).

11. R. D. Poshusta and D. F. Zetick, J. Chem. Phys. 51, 3343 (1969).

12. P. L. Patterson, J. Chem. Phys. 48, 3625 (1968).

13. C. B. Collins and W. W. Robertson, J. Chem. Phys. 40, 701 (1964).

14. R. G. Gordon and Y. S. Kim, J. Chem. Phys., 56, 3122 (1972).

15. G. Knop and W. Paul in: Alpha, Beta, and Gamma-Ray Spectroscopy (ed. Kai Siegbahn, North-Holland Co., Amsterdam, 1965) p. 1-25.

16. M. Bourene and J. Le Calve, Le Journal De Physique, 32, 29 (1971).

17. D. K. Bohme, N. G. Adams, M. Mosesman, D. B. Dunkin and E. E. Ferguson, J. Chem. Phys. 52, 5094 (1970).

18. D. Villarejo, R. R. Herm and M. G. Inghram, J.O.S.A. 56, 1574 (1966).

19. H. J. Oskam, Philips Res. Rept., 13, 335 (1958).

20. R. A. Gerber, G. F. Sauter and H. J. Oskam, Phys. Lett., 19, 656 (1966).

21. R. A. Gerber and M. A. Gusinow, Phys. Rev. A4, 2027 (1971).

22. F. C. Fehsenfeld, P. D. Goldan, A. L. Schmeltekopf, H. I. Schiff, and E. E. Ferguson, J. Chem. Phys. 44, 4087 (1966).

23. C. B. Collins and A. J. Cunningham, The Nitrogen Ion Laser, Fifth Semi-Annual Technical Report, UTDP-ML-02 (1974).

24. R. V. Lovelace and R. M. Sudan, Phys. Rev. Lett. 27, 1256 (1971).